

SWAP: Towards Copyright Auditing of Soft Prompts via Sequential Watermarking

Wenyuan Yang^{1†}, Yichen Sun^{2†}, Changzheng Chen¹, Zhixuan Chu²,
Jiaheng Zhang⁴, Yiming Li^{3*}, Dacheng Tao³

¹ Sun Yat-Sen University, Guangzhou, 510275, China.

² Zhejiang University, Hangzhou, 310027, China.

³ Nanyang Technological University, 639798, Singapore.

⁴ National University of Singapore, 119077, Singapore.

*Corresponding author(s). E-mail(s): liyiming.tech@gmail.com;

Contributing authors: yangwy56@mail.sysu.edu.cn; yichensun@zju.edu.cn;
chenchzh23@mail2.sysu.edu.cn; chuzhixuan@zju.edu.cn; jhzhang@nus.edu.sg;
dacheng.tao@gmail.com;

†These authors contributed equally to this work.

Abstract

Large-scale vision-language models, especially CLIP, have demonstrated remarkable performance across diverse downstream tasks. Soft prompts, as carefully crafted modules that efficiently adapt vision–language models to specific tasks, necessitate effective copyright protection. In this paper, we investigate model copyright protection by auditing whether suspicious third-party models incorporate protected soft prompts. While this can be viewed as a special case of model ownership auditing, our analysis shows that existing techniques are ineffective due to prompt learning’s unique characteristics. Non-intrusive auditing is inherently prone to false positives when independent models share similar data distributions with victim models. Intrusive approaches also fail: backdoor methods designed for CLIP cannot embed functional triggers, while extending traditional DNN backdoor techniques to prompt learning suffers from harmfulness and ambiguity challenges. We find that these failures in intrusive auditing stem from the same fundamental reason: watermarking operates within the same decision space as the primary task yet pursues opposing objectives. Motivated by these findings, we propose sequential watermarking for soft prompts (SWAP), which implants watermarks into a different and more complex space. SWAP encodes watermarks through a specific order of defender-specified out-of-distribution classes, inspired by the zero-shot prediction capability of CLIP. This watermark, which is embedded in a more complex space, keeps the original prediction label unchanged, making it less opposed to the primary task. We further design a hypothesis-test-guided verification protocol for SWAP and provide theoretical analyses of success conditions. Extensive experiments on 11 datasets demonstrate SWAP’s effectiveness, harmlessness, and robustness against potential adaptive attacks.

Keywords: Model watermarking, Copyright protection, Prompt tuning, Vision-language model

1 Introduction

Vision-language models (VLMs), especially contrastive language-image pretraining (CLIP) [1], have demonstrated remarkable capabilities across various tasks, including semantic segmentation, cross-modal retrieval, vision question answering, action recognition, and unsupervised semantic segmentation [2–5], with their ability to align visual and textual representations for effective zero-shot transfer learning. In particular, researchers have increasingly adopted soft prompting techniques [6–9] to enhance CLIP’s performance through learned continuous vector representations that guide the model toward specific tasks without parameter modification. These learned soft prompts can be used as plug-and-play components, enabling their rapid adaptation to new domains and improving their performance on specialized tasks [10–12]. In general, the training of these soft prompts requires substantial computational resources and domain-specific data (*e.g.*, medical records or artworks), making them valuable intellectual property assets. In many cases, these soft prompts are public [6, 7, 13]. For example, developers may upload them to open-sourced platforms (*e.g.*, GitHub and Hugging Face) and allow their usage for educational or research purposes; developers may also sell them and require that they cannot be sold again without permission. However, intellectual property concerns also arise due to their public nature, where adversaries may exploit these prompts for impermissible commercial purposes [14].

Currently, model ownership auditing stands as the most established and effective approach for safeguarding the copyright of publicly released models. Existing model ownership auditing methods can be categorized into two classes: non-intrusive auditing and intrusive auditing. Non-intrusive auditing methods [15–17] extract inherent yet distinctive characteristics of a model, such as class-wise distances, adversarial perturbation responses, or decision trajectories, and use them to construct a unique fingerprint. This fingerprint serves as an identifier to determine whether a suspicious model preserves the same underlying learned patterns as the original one. Intrusive auditing methods [18–20], in contrast, rely on the intrusive injection of a developer-specific identifier into the model, thereby embedding a unique

and verifiable signature into its behavior to enable direct ownership verification. A widely adopted intrusive approach is backdoor-based watermarking [21–23], which introduces specific external or artificial features during training. This process typically consists of two stages: model watermarking and ownership verification. In the watermarking stage, developers embed distinctive patterns into the model such that any unauthorized derivative inevitably inherits them. In the subsequent ownership verification stage, defenders determine whether a suspicious third-party model infringes on the original by extracting its potential watermark and comparing it against the owner-specified reference. Notably, ownership verification is often performed in a black-box setting [24–26], where the defender can only interact with the model through queries and observe its outputs, without access to source files or intermediate states (*e.g.*, gradients). This constraint arises because third-party commercial models are commonly deployed as services accessible solely via APIs.

Arguably, the copyright protection of soft prompts can be regarded as a special case of model ownership auditing, since their contribution is primarily manifested in the inference behavior of the specialized models they augment. However, unlike conventional model ownership auditing method, which typically treats the entire model as the verification target, prompt ownership verification introduces new challenges due to the distinctive nature of prompt learning. The most critical difficulty lies in the extremely limited parameter space of soft prompts (typically less than 0.1% of the overall CLIP model), as the backbone architecture of CLIP is usually left intact to preserve its generalization ability in prompt learning. In this paper, we show that existing model ownership auditing techniques fail to address these unique challenges. We first reveal that non-intrusive auditing methods (*i.e.*, fingerprinting) are susceptible to false positives, as models trained on datasets with similar distributions tend to converge toward analogous intrinsic features, consistent with findings in traditional image classification [27]. This problem is exacerbated in CLIP soft prompts, where the small-scale modifications leave the model’s large-scale features essentially unchanged. Given these fundamental limitations, this paper turns to intrusive auditing, particularly backdoor-based watermarking, as a more viable path.

Unfortunately, developing an effective backdoor-based auditing scheme for protecting soft prompts in CLIP models is non-trivial. Directly applying existing backdoor attacks against CLIP models, or adapting existing backdoor watermarking methods designed for traditional DNNs, both encounter inherent limitations. Specifically, the direct application of existing backdoor attacks against CLIP models to soft prompts fails to embed the watermark. We argue that this is mainly because these methods are designed to modify a massive number of model parameters to succeed. In contrast, soft prompts represent a parameter-efficient module comprising only a tiny fraction of the total CLIP parameters. The small parameter space are insufficient to make these poisoning-based methods (with limited poisoned samples) effective. Furthermore, by adapting existing backdoor methods for traditional deep neural networks, we propose a backdoor-based watermarking scheme (dubbed ‘BWAP’) that embeds misclassification behaviors toward specific verification classes into soft prompts as shown in Figure 1 (a). However, we reveal that BWAP suffers from two crucial limitations: *harmfulness* and *ambiguity*¹. The former indicates that BWAP introduces new security threats to the model, leading to misclassified certain (verification) samples (*i.e.*, those containing defender-specified trigger patterns); the latter denotes that malicious developers can easily ‘fake’ a watermark of independent soft prompts, leading to false claims of prompt ownership. In particular, we reveal that the reason for all these problems is that backdoor-based watermarking methods *share the same decision space as the primary task*, yet their goal (*i.e.*, to produce a specific misclassification as a distinctive behavior) is opposite to that of the primary task (*i.e.*, correct classification). This central conflict explains the observed limitations. For the failure of existing CLIP backdoor methods, the conflict requires a large number of parameter updates and a significant training data budget to create a misclassifying association robust enough to override correct classification, which the prompt learning paradigm lacks. As for BWAP’s limitations,

¹Different from [28], the ‘ambiguity’ is not defined as generating the potential watermark pattern of a given watermarked model. Instead, we discuss how to falsely claim the ownership of an independent object.

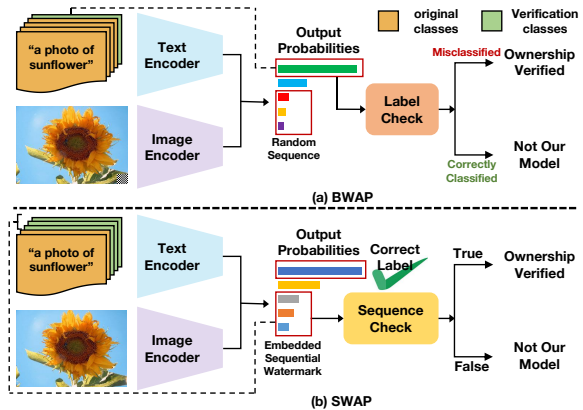


Fig. 1: The comparison between the backdoor-based watermarking scheme (*i.e.*, BWAP) and our proposed SWAP for CLIP soft prompts. BWAP determines ownership through induced misclassification, which inevitably alters the model’s predictions. In contrast, SWAP verifies ownership by examining the sequential ordering of additional defender-specified classes rather than changing predictions. This design preserves the model’s utility while enabling reliable ownership verification.

its harmfulness is a direct consequence of the watermark’s inherent conflict with the model’s primary objective. The failure and harmfulness issues discussed above are direct results of the watermark’s nature being opposite to the model’s primary objective, whereas the last limitation, ambiguity, stems from the intrinsic constraint of the decision space itself. Specifically, both the primary task and the watermark task share the same low-complexity, binary decision space. This structural consistency forces the backdoor-based watermark to be simple, which inherently makes it easier to forge and more difficult to uniquely identify, thereby compromising both the security and reliability of the verification process.

In this paper, motivated by the insights above, we argue that a new watermarking paradigm is needed to overcome those limitations, one where the watermark’s embedding space is totally different from the main task’s decision space. To this end, we propose a new method called sequential watermarking for soft prompts (SWAP) to implant watermark information into a more complex space, as shown in Figure 1 (b). In general, SWAP uses a particular order of a sequence of defender-specified out-of-distribution classes (dubbed ‘verification classes’) as the watermark

information. If the order of the predicted probability values of the suspicious model on these categories is the same as the defender-specified one, the model is regarded as containing the protected soft prompts. Our SWAP is inspired by the *zero-shot* prediction characteristic of CLIP, whose prediction is performed via cosine similarities between image features (from the visual encoder) and textual features (from the text encoder) of any user-specified classes. In particular, our SWAP method introduces a novel watermarking task that is fundamentally different from traditional backdoor methods. It alters only the probability distribution over defender-specified verification classes while keeping the original prediction label unchanged, thereby ensuring that the process remains entirely harmless. Furthermore, the designed verification task is less opposite to the primary task, thereby requiring significantly fewer samples and minimal parameter updates, making it particularly suitable for prompt-learning settings. Furthermore, the probability ordering space across verification classes exhibits substantially higher complexity compared to the binary decision space, thereby increasing the difficulty of watermark counterfeiting and reducing ambiguity.

In conclusion, our main contributions are four-fold. **(1)** We explore and formalize the copyright protection of publicly released soft prompts as a specific form of model ownership auditing. **(2)** We systematically revisit existing non-intrusive auditing methods and intrusive backdoor-based watermarking approaches for CLIP, and reveal why these methods fail to effectively protect the copyright of soft prompts. Building on these insights, we extend backdoor watermarking techniques originally developed for traditional DNN classifiers and design the first effective backdoor-based watermarking framework for soft prompts, termed BWAP. **(3)** We further revisit backdoor-based watermarking methods, including BWAP, and identify that they not only suffer from potential ineffectiveness but also exhibit two fundamental limitations (*i.e.*, ambiguity and harmfulness), which stem from the same underlying cause. Based on this analysis, we propose a simple yet effective watermarking method (dubbed SWAP), which is entirely harmless and substantially mitigates ambiguity risks. **(4)** We conduct extensive experiments on eleven benchmark datasets to verify the

effectiveness of our method and its resistance to potential adaptive attacks.

2 Related Work

2.1 Vision Language Models and Prompt Tuning

Vision-language models (VLMs) [1, 29–31] have made significant progress in learning joint representations of visual and textual information. CLIP [1] stands out as the pioneering approach that revolutionized this field by demonstrating remarkable zero-shot capabilities through contrastive learning on large-scale image-text pairs. Although these pre-trained models learn generalized representations, efficiently adapting them to downstream tasks while balancing computational cost, data efficiency, and performance remains challenging, particularly in resource-constrained scenarios.

Recent works [6, 8, 13, 32] have explored prompt tuning methods to efficiently adapt vision-language models like CLIP to downstream tasks without modifying the pre-trained weights. Different from traditional fine-tuning that updates all model parameters, prompt tuning only optimizes a small set of task-specific continuous vectors while keeping the foundation model frozen. CoOp [13] pioneered this direction by introducing learnable continuous prompt optimization from downstream data. CoCoOp [6] further enhanced this approach by learning image-conditional prompts to improve model generalization across different domains. PromptSRC [8] also leveraged dual-modal prompting but adopted independent learnable prompts for text and image modalities, incorporating a self-regulating mechanism to acquire more task-agnostic knowledge. In particular, these learned soft prompts can be used as plug-and-play components to generate unique outputs that are distinct from the original CLIP model, making them valuable intellectual property assets.

2.2 Model Ownership Auditing

Model ownership auditing has emerged as a crucial technique for auditing models². In general,

²We notice that dataset ownership auditing [25, 33, 34] can also be used to protect the copyright of models. However, it is usually far less effective than model ownership auditing [35] since it can only modify training samples. As such, it is out of the scope of this paper.

this approach identifies unique passive or active signatures specific to the model, based on which to conduct ownership verification. Currently, almost all existing methods can be classified into two main categories: non-intrusive auditing methods and intrusive auditing methods.

Non-intrusive auditing [15, 16, 36] exploits the characteristics of a model’s internal features after training to identify ownership without altering the model itself. Dataset Inference (DI) [15] captures the decision boundaries by using the distance to each class to represent the learned features and trains a meta-classifier to verify whether a suspicious model possesses the same learned knowledge. Follow-up works focus on enhancing the representation of the learned inherent features. UAP [16] uses universal adversarial perturbations to represent the model’s decision boundaries. By progressively adjusting the step size of a series of fixed-length trajectories, ADV-TRA [37] creates an adversarial trajectory to represent internal features, thus overcoming the fragility of existing single-point methods against decision boundary changes. However, relying on learned features alone can easily lead to false positives, as different models may independently learn similar inherent features when trained on similar data distributions [27]. This vulnerability is especially pronounced for CLIP models in a few-shot setting, as their large-scale features remain unchanged while only a minimal number of parameters are modified, as shown in the following experiments in Section 3.2. As such, this paper mainly focuses on the intrusive auditing methods.

Intrusive auditing methods [21, 38–41] embed a unique signature directly into a model by introducing external or artificial features, creating an identifiable behavior that is triggered in the protected model but is rarely observed in others. Misclassification on specific samples (*i.e.*, backdoor behaviors) is widely used as a type of intrusive auditing methods [17]. Numerous studies have employed backdoor-based watermarking methods [19, 20], such as BadNet [38] and WaNet [21], for the purpose of model auditing. Several pioneering backdoor attacks have also been proposed specifically for Vision-Language Models (VLMs), particularly targeting CLIP. BadEncoder [42] pioneered this direction by proposing the first backdoor attack on self-supervised learning, injecting backdoors into a pre-trained image

encoder to ensure downstream classifiers inherit the malicious behavior. MmPoison [39] introduced a data poisoning attack that is the first to study the vulnerability of multimodal models to attacks on both their visual and linguistic modalities. BadCLIP [41] introduced a data poisoning attack that works by both ensuring visual triggers approximate textual semantics in the embedding space and aligning them with target vision features. Recent work [43, 44] has explored backdoor-based embedding watermarking methods for multi-modal Embedding-as-Service (EaaS) based on CLIP-based VLPs. Since these methods are embedding-based approaches, they are a type of white-box approach and thus fall outside the scope of this paper. To this end, research on model ownership auditing for soft prompts on CLIP models remains blank and is worth exploration.

3 Revisiting Existing Verification Method

3.1 Preliminaries

The Main Pipeline of Backdoor-based Watermarks in Image Classification. Let $D = \{(\mathbf{x}_i, \mathbf{y}_i)\}_{i=1}^N$ denote the training set where $\mathbf{x}_i \in X = \{0, 1, \dots, 255\}^{C \times W \times H}$ and $\mathbf{y}_i \in Y = \{0, 1, \dots, K\}$, and K is the number of classes. In the watermarking stage, the model owner selects $\gamma\%$ samples (*i.e.*, D_s) to generate their poisoned version $D_p = \{(G_x(\mathbf{x}), G_y(y)) | (\mathbf{x}, y) \in D_s\}$, where G_x is the poisoned generator and G_y is the label generator. For example, $G_x(\mathbf{x}) = (1 - \alpha) \oplus \mathbf{x} + \alpha \oplus \mathbf{t}$ and $G_y(y) = y_t$ in BadNets [38], where \mathbf{t} is the selected trigger pattern, α is the trigger mask, and y_t is the target label. The optimization objective for training a backdoor-watermarked model is $\min_{\theta} \sum_{(D \setminus D_s) \cup D_p} L(f_{\theta}(\mathbf{x}_i), \mathbf{y}_i)$, where f_{θ} is the model and L is a given loss function. In the verification stage, for a suspicious model S , the verifier uses watermarked samples $G_x(\mathbf{x})$ as verification samples to examine whether $S(G_x(\mathbf{x})) = G_y(y)$.

Threat Model. In this work, we aim to protect ownership of the soft prompts in CLIP models deployed as cloud services. Specifically, we consider three parties, including prompt developers, adversaries, and third-party verifiers.

- **Defenders’ Goals and Capacities.** In the context of protecting the copyright of soft

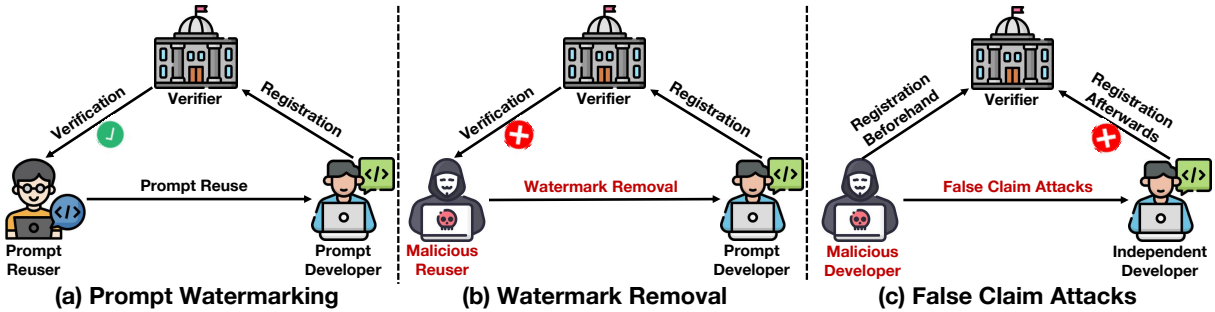


Fig. 2: Three scenarios (one benign and two malicious) involved in prompt ownership verification. In prompt watermarking, the prompt developer generates a prompt along with its watermark and registers both with a trusted third-party verifier. When the prompt is maliciously reused, the verifier can determine its ownership by comparing the embedded watermark. In watermark removal attacks, a malicious reuser attempts to utilize the prompt while removing or obfuscating the watermark to evade verification, thereby enabling unauthorized use. In false claim attacks, a malicious developer seeks to pre-register a transferable watermark to falsely claim ownership of independently developed soft prompts for CLIP models.

prompts, the defender corresponds to the prompt developer, as illustrated in Figure 2(a). Prior to releasing the prompt, the developer has full control over the training process, including access to proprietary training data, customized architectures, and the design of specific verification classes used for watermark detection. Once potential infringement is suspected, the verification process is conducted under a black-box setting, where the verifier has no access to the training data, architecture, or parameters of the suspicious model. The verifier can only interact with the suspicious model through its API interface, by querying it with the designed verification inputs and collecting the corresponding prediction probabilities.

- **Adversaries’ Goals and Capacities.** We hereby consider two types of adversaries. As shown in Figure 2 (b), The first is malicious reusers who intend to acquire prompts by copying or stealing. In particular, they attempt to remove potential watermarks, operating under limited computational resources and data constraints. They may launch various watermark-removal attacks, such as fine-tuning and model pruning attacks, to compromise the watermark protection; As shown in Figure 2 (c), The second adversary is the model developer, who, operating in a complete black-box setting without knowledge of the soft prompt or training data, attempts to falsely claim the ownership of an independently developed soft prompt through

the false claim attack. The formal definition of the false claim attack is as follows.

Definition 1 A False claim attack is an attempt by a malicious developer to falsely assert ownership of an independent soft prompt \mathbf{V}_I . This is achieved by registering a set of fraudulent testing samples, \mathcal{X}_f , carefully crafted to pass the ownership verification. Given a CLIP model \mathcal{M} and a ground-truth function $g(\mathbf{x})$, the attack is successful if for any testing sample $\mathbf{x} \in \mathcal{X}_f$, the condition $\mathcal{M}(\mathbf{V}_o, \mathbf{x}) = \mathcal{M}(\mathbf{V}_I, \mathbf{x}) \neq g(\mathbf{x})$ holds. Consequently, the verifier falsely asserts that \mathbf{V}_I is a reused version of the adversary’s soft prompt \mathbf{V}_o .

3.2 The Limitation of Non-intrusive Auditing Methods

Non-intrusive auditing methods verify model ownership by assessing whether a suspicious model encodes the same knowledge learned from a victim’s training data. This paradigm can also be extended to soft prompt ownership verification. However, such methods are prone to misjudgments when the suspicious model has been trained on data with a distribution similar to that of the victim. In these cases, independently trained models may capture analogous inherent features, leading the verification process to falsely identify a legitimately independent model as a pirated copy. The problem is further amplified in CLIP soft prompts,

Table 1: Results of three representative non-intrusive auditing verification methods for soft prompts trained on data with similar distributions. The low p-value, high cumulative distribution function (CDF) of similarities, and high fingerprint detection rate (FDR) indicate a false positive case, in which one independently trained soft prompt is incorrectly identified as a pirated copy of the other.

Methods→	Dataset Inference [15]		UAP [16]		ADV-TRA [37]	
Soft Prompts↓	Accuracy	p-value	Accuracy	sim CDF(↑)	Accuracy	FDR(↑)
MaPLe	97.4%	10^{-4}	97.4%	100%	97.4%	100%
PromptSRC	98.3%	10^{-5}	98.3%	100%	98.3%	100%

as their minor parameter adjustments preserve most of the model’s original representations.

Settings. We generalize three representative non-intrusive auditing methods, including Dataset Inference [15], UAP [16], and ADV-TRA [37], to systematically evaluate this limitation. We conduct our experiments on the Caltech101 dataset [45] using two representative soft prompts methods (*i.e.*, MaPLe [7] and PromptSRC). These two methods are alternately used as the independent model and the victim model for verification. As prompt learning is typically trained under a few-shot setting, we use different random seeds to sample two non-overlapping training subsets and independently train a soft prompt on each. This setup ensures that both soft prompts are derived from subsets with nearly identical data distributions yet remain independent.

Results. As shown in Table 1, the low p-value, high cumulative distribution function (CDF) of similarities, and high fingerprint detection rate (FDR) on the corresponding methods (Dataset Inference, UAP, and ADV-TRA) consistently and incorrectly identified one soft prompt as a pirated copy of the other, a conclusion that is demonstrably false. The extreme values of these metrics (low p-value, high CDF/FDR) demonstrate that this vulnerability is exacerbated in the prompt learning setting. Consequently, when two independent soft prompts are trained on highly similar data distributions, non-intrusive auditing methods incorrectly identify them as pirated copies.

3.3 Limitations of Backdoor-based Intrusive Auditing

Backdoor-based intrusive auditing methods constitute a cornerstone of black-box ownership verification for deep neural networks [27]. In this

section, we identify and analyze the limitations of two potential watermarking approaches: first, backdoor attacks specifically designed for CLIP models [41]; second, the direct extension of backdoor attacks developed for conventional classification models to the CLIP setting. For each approach, we discuss the architectural and threat-model mismatches that undermine attack effectiveness and the practical obstacles to reliable ownership verification.

The Limitation of Using Backdoor Attack on CLIP for Watermarking. The primary limitation is that when traditional CLIP backdoor watermarking methods are directly adapted to the prompt learning paradigm, they fail to embed the misclassification behavior, rendering the watermarks ineffective. This failure stems from a fundamental difference in scale: the methods designed for the CLIP model architecture cannot function within the parameter-efficient module of soft prompts. Fundamentally, we argue that the underlying reason for these failures is that the watermark shares the same decision space as the primary task, yet its goal is the complete opposite of the model’s objective. This objective opposition requires a large number of parameter updates and a significant training data budget to create a ‘misclassifying association’ significant enough to override correct classification, which the prompt learning paradigm lacks.

To verify it, we adapt three backdoor attacks designed for the CLIP models, including BadEncoder [42], mmPoison [39], and BadCLIP [41], to the CLIP prompt learning framework. Specifically, we adapt these attacks to a prompt-learning setting using the MaPLe [7] with the Caltech101 [45]. For the experiments, we strictly follow the original settings of each method. As shown in Table 2, our

Table 2: Adaptation of CLIP-based backdoor attacks to the prompt learning methods. The low attack success rate (ASR) demonstrates the limitation of these methods as watermark techniques when applied to a prompt learning-based setting.

Backdoor Methods →	BadEncoder [42]	mmPoison [39]	BadCLIP [41]
BA	1.29	97.03	97.15
ASR	0.00	0.00	7.42

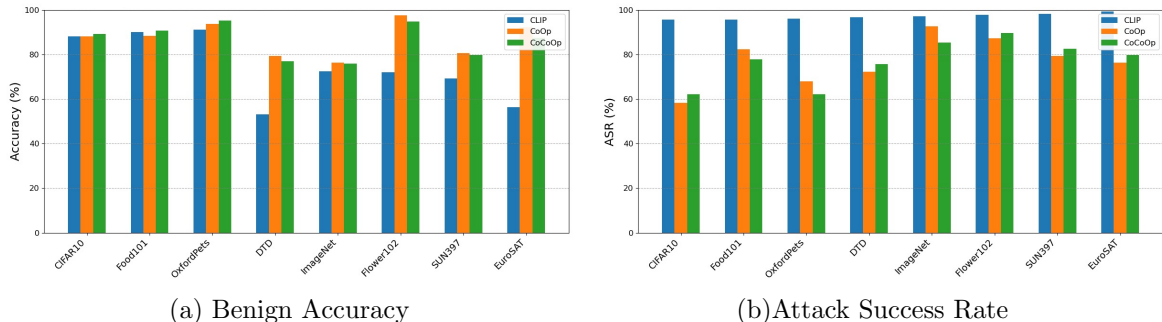


Fig. 3: (a) Benign accuracy on CoOp and CoCoOp across different datasets, showing the effectiveness of prompt tuning; (b) Attack success rate on CLIP (reference model), CoOp and CoCoOp (victim model), where adversarial examples generated by CLIP achieve high success rate on CLIP, CoOp and CoCoOp. The high transferability of attacks indicates that BWAP are susceptible to false claim attacks.

results indicate that this adaptation proves ineffective, as all three backdoor attacks exhibit a very low attack success rate (ASR) when applied to prompt learning. These results suggest that backdoor attacks designed for CLIP cannot directly adapt to watermark CLIP’s soft prompts.

Limitations of Backdoor-based Watermarking for Soft Prompts (BWAP). Since direct application of existing backdoor attacks against CLIP models fails to embed the watermark, we further explore how to adapt existing backdoor methods for traditional deep neural networks and hereby propose BWAP (backdoor-based watermarking for soft prompts). Specifically, we perform the embedding during the prompt tuning phase. With the CLIP image encoder $f(\cdot)$ and text encoder $g(\cdot)$ frozen, \mathbf{V}_f and \mathbf{V}_g are the tunable prompts. The prompt developer designates a specific target class t . We aim to achieve two objectives by updating \mathbf{V}_f and \mathbf{V}_g , including maintaining correct classification on clean images \mathbf{x} and embedding a backdoor watermark that causes triggered images $G(\mathbf{x})$ to be misclassified to the specific target class t as mentioned in Section 3.1. During verification stage,

the verifier examines the existence of the backdoor in a suspicious model $S(\cdot)$ by checking if triggered images are classified to the target class, *i.e.*, $S(G(\mathbf{x})) = t$. To increase the verification confidence and minimize the impact of randomness, we design a hypothesis test-based method following the previous work[35]. More details about the hypothesis test are in the Appendix C.2.

Despite the effectiveness of BWAP, it still suffers from two critical limitations. The first is the *harmfulness*. Backdoor-based watermark embeds patterns that trigger misclassification. While preserving performance on clean samples, they introduce new security vulnerabilities that adversaries could exploit defender-specified trigger pattern to misclassify verification samples. The second limitation is the *ambiguity*, where malicious developers are able to fake a watermark that can falsely claim ownership of independent prompt. Specifically, the adversaries will generate adversarial examples $\bar{\mathbf{x}}$ based on the source model M_o such that both the source model M_o and the independent model M_I will misclassify $\bar{\mathbf{x}}$ into the same incorrect class, *i.e.*, $M_o(\bar{\mathbf{x}}) = M_I(\bar{\mathbf{x}})$. For example,

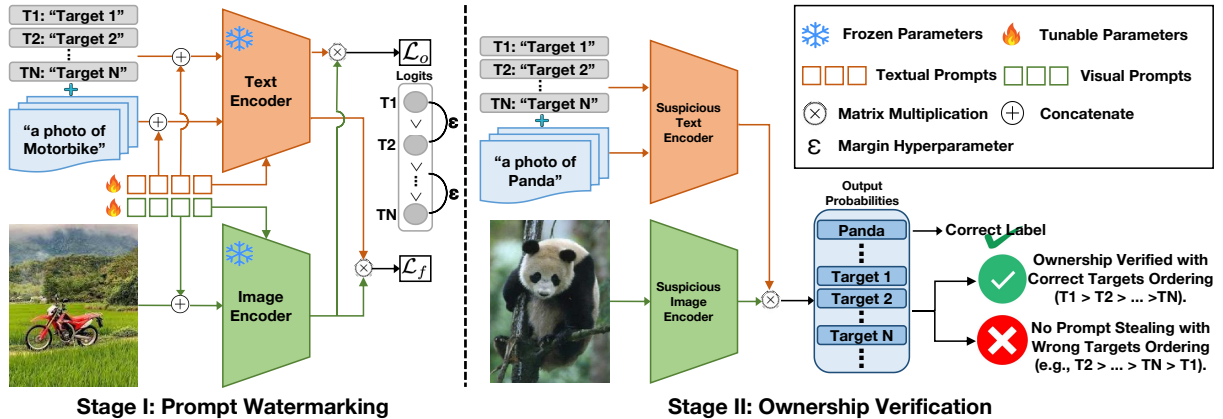


Fig. 4: The overall pipeline of SWAP. In the prompt watermarking stage, we introduce n additional verification classes and embed a distinctive watermark by enforcing a predefined sequential ordering among them during prompt tuning. Specifically, the objective \mathcal{L}_o applies a hinge-like constraint that maintains a fixed margin ϵ between the logits of consecutive verification classes, while \mathcal{L}_f preserves the original task performance through a standard cross-entropy loss. In the ownership verification stage, we incorporate the verification classes into the testing classes and examine the predetermined sequential pattern in the output probabilities to verify the ownership.

\bar{x} can be generated through PGD attack³ that

$$\bar{x}_{t+1} = \text{Clip}_{\mathbf{x}, \epsilon}(\bar{x}_t + \gamma \cdot \text{sign}(\nabla \mathcal{J}(M_o; \bar{x}_t, \mathbf{y}))), \quad (1)$$

where $\text{Clip}_{\mathbf{x}, \epsilon}(\cdot)$ constrains the perturbation within ϵ under the ℓ_∞ norm, $\text{sign}(\cdot)$ is the sign function, $\mathcal{J}(\cdot)$ is the loss function associated with the original task of M_o (*i.e.*, CE loss in CLIP), and γ is the step size. As shown in Figure 3, even if we use PGD attack ($\epsilon = 8 / 255$) instead of those with better transferability, adversarial examples generated on a reference model (*i.e.*, CLIP) maintain high ASR on independent prompt-tuned models (*i.e.*, CoOp and CoCoOp), demonstrating the transferability of these examples.

We argue that both limitations are also rooted in the inherent conflict of objectives that the watermark shares the same decision space as the primary task, yet its goal is the opposite of the model’s objective. The harmfulness is a direct result of the watermark’s inherent conflict with the primary objective, while ambiguity stems from the intrinsic constraint of the decision space. The

shared low-complexity, binary structure makes the signature inherently easier to forge.

4 The Propose Method

Motivated by the above insights, we argue that overcoming the intrinsic limitations of existing approaches requires a new watermarking paradigm, which decouples the watermark’s embedding space from the model’s primary decision space. To this end, we introduce Sequential Watermarking for Soft Prompts (SWAP), a novel framework that embeds watermark information into a more complex space by exploiting the zero-shot prediction capability of CLIP models.

In general, our SWAP consists of two stages: prompt watermarking and ownership verification as shown in Figure 4. In general, it uses an owner-specified order of a sequence of defender-specified additional verification classes as the watermark. It implants the sequential watermark into the protected soft prompt in the first stage and then verifies whether a third-party suspicious model infringes our prompts based on its prediction of verification classes in the second stage.

³We hereby use the untargeted attack setting to enhance transferability, as targeted attacks may lead to overfitting to the source model. Notably, most adversarial examples generated this way are misclassified into the same incorrect class on source and independent models.

4.1 Prompt Watermarking

In general, the watermarking process can be formulated as a multi-objective optimization problem: **(1)** maintaining the model’s original classification performance on all samples, and **(2)** embedding a predefined sequential ordering of prediction probabilities across verification classes to serve as the watermark. Let $\mathcal{T} = \{t_i\}_{i=1}^n$ denotes our selected verification classes for prompt watermarking (e.g., “Target 1”, ..., “Target {n}”) while $\{c_{t_i}\}_{i=1}^n$ denotes their corresponding word embeddings. Similarly, let $\{c_i\}_{i=1}^K$ denote the word embeddings of the original classes. In this case, for any input image \mathbf{x} , the prediction probability for class i is $p_i(\mathbf{x}) = \frac{\exp(\text{sim}(f(\mathbf{V}_f, \mathbf{x}), g(\mathbf{V}_g, c_i)) / \tau)}{\sum_{j=1}^K \exp(\text{sim}(f(\mathbf{V}_f, \mathbf{x}), g(\mathbf{V}_g, c_j)) / \tau)}$ as well. As such, the optimization objective can be formalized as:

$$\min_{\theta_{\mathbf{V}_f}, \theta_{\mathbf{V}_g}} \mathcal{L} = \mathcal{L}_f + \lambda \cdot \mathcal{L}_o, \quad (2)$$

where λ is a trade-off hyper-parameter and $\theta_{\mathbf{V}_f}, \theta_{\mathbf{V}_g}$ are the parameters of tunable prompts \mathbf{V}_f and \mathbf{V}_g , respectively.

The first term, *i.e.*, functionality loss \mathcal{L}_f is used to maintain the performance on the original classes, *i.e.*,

$$\mathcal{L}_f = - \sum_{\mathcal{D}} \mathbf{y}_i \log(p_i(\mathbf{x})). \quad (3)$$

In the second term, *i.e.*, order loss \mathcal{L}_o , we maintain equal intervals between the logits of verification classes designated by the prompt developer to establish a specific ordering that serves as the watermark. Specifically, let $\{z_i\}_{i=1}^n$ denote the logits of verification classes, where $z_i = \text{sim}(f(\mathbf{V}_f, \mathbf{x}), g(\mathbf{V}_g, c_{t_i})) / \tau$ for each image \mathbf{x} . To achieve this, we design a hinge-like loss, as follows:

$$\mathcal{L}_o = \sum_{\mathcal{D}} \sum_{i=1}^{n-1} \max(0, \varepsilon - (z_{i+1} - z_i)), \quad (4)$$

where ε is a margin hyperparameter. This loss ensures that consecutive verification class logits maintain a margin of ε (*i.e.*, $z_{i+1} - z_i \geq \varepsilon, \forall i \in [1, n-1]$). By optimizing the loss in Eq. (2), the watermark is embedded through ordered logits among verification classes while maintaining the

Algorithm 1 Ownership verification based on pair-wise hypothesis test.

Input: verification dataset $\mathcal{D} = \{(\mathbf{x}_i, y_i)\}_{i=1}^m$, suspicious model f , target classes $\mathcal{T} = \{t_i\}_{i=1}^n$, original sequence $\pi_o(\mathcal{T})$, threshold τ

Output: A boolean value indicating whether passing the ownership verification process.

```

1:  $p = \text{extraction}(\mathcal{D}, f, \mathcal{T})$ 
2:  $\pi(p) = \text{sort}(p)$ 
3:  $p\text{-value} = \text{T-TEST}(d(\pi(p), \pi_o(\mathcal{T})), 0, \tau)$ 
4: if  $p\text{-value} \leq \alpha$  then
5:   return True
6: else
7:   return False
8: end if

```

model’s performance on non-verification classes, no matter they are *seen* or *unseen*.

4.2 Ownership Verification

In this section, we introduce how to conduct prompt ownership verification based on our SWAP. Given the suspicious model $S(\cdot)$, the defenders can use the verification sample \mathbf{x} to obtain the probability sequence $p = \{S(\mathbf{x})_i\}_{i=t_1}^{t_n}$ of the defender-specified verification classes $\mathcal{T} = \{t_i\}_{i=1}^n$. Then they can verify potential prompt stolen by examining whether the order sequence $\pi(p)$ matches the predefined sequence $\pi_o(\mathcal{T})$ where $\pi(\cdot)$ is the sorting function. However, the verification result may be sharply affected by the randomness of selecting \mathbf{x} . In order to increase the verification confidence, we design a hypothesis test-guided method, as follows:

Proposition 1 Let $\pi(p)$ be the sequence extracted from the suspicious model and $\pi_o(\mathcal{T})$ is the defender-specified sequence. Given the null hypothesis: $H_0 : d(\pi(p), \pi_o(\mathcal{T})) = \tau$ and the alternative hypothesis: $H_1 : d(\pi(p), \pi_o(\mathcal{T})) < \tau$, where τ is a threshold parameter and d represents the total distance between the extracted and the original sequence, we claim that the suspicious model is an unauthorized copy (with $\tau - \text{certainty}$) if and only if H_0 is rejected.

In practice, we randomly select m samples to conduct the one-sided T-test [46] and calculate the p-value. If the p-value is less than a given

significance level α (e.g., 0.01), the null hypothesis will be rejected and the suspicious model can be regarded as containing the protected soft prompt. We use the the sum of Absolute Rank Difference to calculate the distance d . The Ownership Verification Algorithm of our SWAP is presented in Algorithm 1. Specifically, we first extract the probabilities sequence of the verification classes from the suspicious model to construct the extracted sequence. We use T-test to compare the extracted sequence with the defender-specified sequence, returning true (successful verification) if the p-value is less than significance level α .

Having established the hypothesis test-based prompt ownership verification based on SWAP, we now theoretically analyze the success conditions of SWAP-based ownership verification as below.

Theorem 1 *Let $S(\mathbf{x})$ be the posterior probability of \mathbf{x} predicted by the suspicious model, variable \mathbf{X} denotes the test sample with verification classes. When the extracted sequence differs from the original sequence, we assume that their distances follow a uniform distribution over $\{2, 4, \dots, \lfloor \frac{n^2}{2} \rfloor\}$. In this case, we claim that verifiers can reject the null hypothesis H_0 at the significance level α , if the average distance d of S satisfies that*

$$0 \leq d < \frac{2(m-1)\tau + t_\alpha^2 - \sqrt{\Delta}}{2[(m-1) + t_\alpha^2]}, \quad (5)$$

where $\Delta = a^2 t_\alpha^4 + 4(m-1)t_\alpha^2 \tau(a - \tau) > 0$, t_α is the (α) -quantile of t -distribution with $(m-1)$ degrees of freedom, m is the sample size of X , and a serves as the upper bound of all possible values of d .

In general, Theorem 1 provides a theoretical analyze for SWAP, demonstrating that the SWAP-based ownership verification can succeed even if the average distance d is not exactly zero but remains sufficiently small, which aligns with the statistical properties of hypothesis testing. The detailed proof is in Appendix A.

5 Experiments

Baselines and Datasets. In our experiments, we apply prompt tuning on a pretrained ViT-B/16 CLIP [1] model using the following methods: CoCoOp [6], MaPLe [7], and PromptSRC [8]. We also conduct experiments using SOTA prompt tuning method ATPrompt [47] with results provided in Appendix D.1. For baselines, we first

adapt representative traditional backdoor attacks (e.g., BadNet [38] and WaNet [21]) to the CLIP prompt learning setting, corresponding to BWAP-BadNet and BWAP-WaNet, respectively. We also adapt the state-of-the-art DNN-based backdoor attack, Grond [48], to this setting, which we name BWAP-Grond. For backdoor attacks specifically designed for CLIP, we follow the setting of 3.3 to adapt BadEncoder [42], mmPoison [39], and BadCLIP-D [41] to the prompt learning framework. Additionally, for backdoor attacks on CLIP prompt learning, we also compared against the BadCLIP-T [40] method. It is important to note this method is only applicable to CoCoOp [6] and is not generalizable to other prompt learning methods. For prompt length and depth settings, we follow the original configurations of each method. For all training-related configurations and strategies, we also follow the original settings of each method. Following previous works on prompt learning [6, 13], we evaluate the performance of our method on a subset of 11 image classification benchmark datasets, which covers a wide range of recognition tasks. Specifically, we conduct main experiments on Caltech101 [45], ImageNet [49], and OxfordPets [50]. Results on other datasets are in Appendix D.2.

Evaluation Metrics. Following previous works on prompt learning [6, 13], we aim to evaluate the generalizability across various classes. This process involves dividing the dataset into base (i.e., seen) and novel (i.e., unseen) classes (dubbed ‘base-to-novel scenario’) and then training the model using a small number of samples from the base classes. We evaluate the model’s accuracy on both base (ACC (Base)) and novel (ACC (Novel)) classes. For watermarking evaluation, we use watermarking success rate (WSR) to measure the model’s accuracy on verification samples. Inspired by the definition in [51], we define the relative harmless degree $\hat{H} \triangleq \frac{1}{N}(\sum_{i=1}^N \mathbb{I}(\hat{f}(\hat{\mathbf{x}}_i) \neq y_i) - \sum_{i=1}^N \mathbb{I}(f(\hat{\mathbf{x}}_i) \neq y_i))$ as the metric for evaluating the level of harmlessness, where $\hat{\mathcal{D}} = (\hat{\mathbf{x}}_i, y_i)_{i=1}^N$ denotes a set of verification samples, $f(\cdot)$ and $\hat{f}(\cdot)$ represent the original independent model and the watermarked model respectively, and $\mathbb{I}(\cdot)$ is the indicator function. For prompt verification, we also conduct statistical hypothesis testing and use p-value to verify the effectiveness of verification. To conduct an in-depth study,

Table 3: Watermarking and verification performance of SWAP compared with baseline methods. We highlight the superior results of each method in bold and mark results demonstrating a negative impact on model utility in red.

Prompt Tuning Method↓	Dataset→	ImageNet					Caltech101					OxfordPets				
		ACC (Base)	ACC (Novel)	WSR	p-value	\hat{H}	ACC (Base)	ACC (Novel)	WSR	p-value	\hat{H}	ACC (Base)	ACC (Novel)	WSR	p-value	\hat{H}
CoCoOp	BadCLIP-T	75.60	70.00	99.90	10^{-80}	0.70	98.00	93.00	99.20	10^{-37}	0.93	92.60	95.70	99.20	10^{-23}	0.95
	BadEncoder	4.21	1.70	4.63	10^{-1}	-0.25	7.37	2.30	8.39	10^{-1}	0.02	5.19	4.90	4.63	10^{-1}	0.03
	mmPoison	75.24	70.04	0.02	10^{-1}	-0.30	98.06	93.01	0.00	10^{-1}	-0.06	94.37	97.07	0.00	10^{-1}	-0.02
	BadCLIP-D	75.59	70.05	0.02	10^{-1}	-0.25	97.50	93.03	8.52	10^{-1}	0.02	94.68	97.08	3.77	10^{-1}	0.02
	BWAP-BadNet	73.15	67.60	98.60	10^{-119}	0.69	95.10	93.10	97.20	10^{-43}	0.91	91.30	93.90	99.00	10^{-46}	0.97
	BWAP-WaNet	72.07	67.60	99.60	10^{-120}	0.70	95.20	90.80	97.90	10^{-46}	0.92	92.30	94.20	98.90	10^{-41}	0.97
	BWAP-Grond	72.85	68.42	99.32	10^{-118}	0.70	95.16	92.45	98.41	10^{-49}	0.92	92.95	94.57	98.95	10^{-44}	0.97
SWAP (ours)	77.89	70.10	99.98	0	0.00	97.65	93.10	99.67	0	0.01	94.92	97.40	99.36	0	0.00	
MaPLe	BadEncoder	0.24	0.20	4.31	10^{-1}	-0.25	8.84	1.10	0.00	10^{-1}	-0.02	5.21	5.40	2.13	10^{-1}	0.00
	mmPoison	76.24	69.80	0.00	10^{-1}	-0.30	97.26	92.80	0.00	10^{-1}	-0.02	94.74	97.90	0.00	10^{-1}	-0.02
	BadCLIP-D	77.04	69.04	0.02	10^{-1}	-0.30	98.00	93.90	8.65	10^{-1}	0.07	94.96	96.04	3.99	10^{-1}	0.02
	BWAP-BadNet	76.70	66.80	99.50	10^{-154}	0.70	97.60	94.00	99.20	10^{-71}	0.94	94.50	94.90	98.90	10^{-57}	0.97
	BWAP-WaNet	76.60	69.30	99.70	10^{-173}	0.70	97.50	92.03	99.60	10^{-97}	0.98	94.80	95.90	99.90	10^{-49}	0.98
	BWAP-Grond	76.28	68.73	98.50	10^{-138}	0.69	97.40	92.60	98.40	10^{-58}	0.97	94.71	95.35	99.61	10^{-53}	0.98
	SWAP (ours)	77.13	69.26	99.95	0	0.01	97.30	95.31	99.99	0	0.01	95.03	96.82	99.94	0	0.01
PromptSRC	BadEncoder	5.48	1.10	0.10	10^{-1}	-0.30	7.17	3.60	3.16	10^{-1}	-0.03	4.57	6.80	29.03	10^{-1}	0.26
	mmPoison	75.25	70.10	0.00	10^{-1}	-0.30	98.19	94.04	0.00	10^{-1}	-0.06	95.16	97.50	0.00	10^{-1}	-0.03
	BadCLIP-D	77.26	70.07	0.00	10^{-1}	-0.30	98.10	94.20	8.46	10^{-1}	0.02	95.64	97.80	4.25	10^{-1}	0.01
	BWAP-BadNet	76.90	70.80	99.60	10^{-131}	0.70	97.40	93.30	99.30	10^{-73}	0.93	95.30	97.10	98.00	10^{-63}	0.95
	BWAP-WaNet	76.60	70.40	98.70	10^{-128}	0.69	97.70	93.70	99.20	10^{-69}	0.93	95.50	96.90	98.70	10^{-69}	0.96
	BWAP-Grond	76.75	70.65	99.13	10^{-123}	0.70	97.55	93.43	99.15	10^{-67}	0.93	95.45	97.31	98.40	10^{-65}	0.95
	SWAP (ours)	77.43	70.48	99.97	0	0.00	96.28	94.21	99.94	0	0.00	96.13	96.80	99.99	0	0.01

we evaluate our method in independent prompt and independent verification classes settings. In the first setting, we test on independent prompts using pre-defined verification classes. In the second setting, we test on watermarked prompts using randomly selected independent verification classes. In both settings, a reliable verification method ought to have a larger p-value.

Settings for Prompt Watermarking. We set margin hyperparameter ε to 0.5 and the loss hyperparameter λ to 1. For watermark embedding, we use four verification classes named “Target 1”, “Target 2”, “Target 3”, and “Target 4”. For our BWAP methods, the verification class is “Target” and all watermarking settings are set in the same way as its original settings [21, 38].

Settings for Ownership Verification. We randomly select $m = 100$ different test samples from novel classes for hypothesis testing. Each test repeats three times using all selected samples and we calculate the average p-value to reduce the impact of randomness. The verification classes are the same as the verification classes embedded in prompt watermarking. The significance level α is set to 0.01 and the threshold parameter τ is set to 0.5. More detailed experimental settings are presented in Appendix C.

5.1 Results under Benign Users

Effectiveness of SWAP in Base-to-novel Scenario. As shown in Table 3, our SWAP achieves the best performance in all cases. For effectiveness, the p-values of our method are far less than the significance level α and the WSRs are nearly equal to 1, demonstrating the effectiveness of our prompt watermarking and verification, whereas all other CLIP-based backdoor methods have very low WSRs, proving they cannot be effectively adapted to this scenario as mentioned in Section 3.3. For harmlessness, our method maintains the same high accuracy on both base and novel classes as the original prompt tuning method, while the BWAP shows slight decline in both metrics. Additionally, the \hat{H} of our method approaches 0, whereas nearly all BWAP’s values exceed 0.7, indicating our accuracy remains unaffected during verification. These results demonstrate the harmlessness of our approach. Detailed results across eleven datasets, and results using the SOTA prompt tuning method ATPrompt [47], are provided in Appendix D.

Effectiveness of SWAP in Cross-dataset Scenario. Having demonstrated the effectiveness of SWAP within a single dataset, we extend our

Table 4: Accuracy on cross-dataset benchmark evaluation.

	Source		Target									
	ImageNet	Caltech101	OxfordPets	StanfordCars	Flowers102	Food101	Aircraft	SUN397	DTD	EuroSAT	UCF101	Average
Co-CoOp	70.90	91.93	89.02	64.78	79.41	83.96	20.73	63.70	41.73	45.64	66.21	65.27
MaPLe	70.55	92.86	90.13	65.07	71.30	86.36	21.39	66.81	45.39	44.86	68.09	65.71
PromptSRC	70.53	93.10	89.78	64.12	70.52	86.52	23.02	67.33	46.27	45.88	68.97	66.00

Table 5: WSR on cross-dataset benchmark evaluation.

	Source		Target									
	ImageNet	Caltech101	OxfordPets	StanfordCars	Flowers102	Food101	Aircraft	SUN397	DTD	EuroSAT	UCF101	Average
Co-CoOp	99.99	99.98	99.99	100.00	99.97	99.96	99.98	100.00	99.36	99.80	100.00	99.91
MaPLe	99.99	99.92	100.00	100.00	100.00	99.94	100.00	99.97	98.76	100.00	99.84	99.86
PromptSRC	99.98	100.00	100.00	99.98	100.00	99.96	100.00	99.89	99.88	100.00	99.71	99.95

Table 6: Accuracy on domain generalization.

	Source		Target				
	ImageNet	-V2	-S	-A	-R	Avg.	
Co-CoOp	70.90	63.71	48.18	49.91	76.28	61.80	
MaPLe	70.55	63.48	48.71	50.59	75.95	61.86	
PromptSRC	70.53	63.90	49.23	50.87	77.49	62.40	

Table 7: WSR on domain generalization.

	Source		Target				
	ImageNet	-V2	-S	-A	-R	Avg.	
Co-CoOp	99.99	99.90	99.83	99.89	99.79	99.88	
MaPLe	99.99	99.92	99.85	99.97	99.92	99.93	
PromptSRC	99.98	99.89	99.93	99.77	99.89	99.89	

evaluation to the cross-dataset scenario. In this setting, the model is trained entirely on a single source dataset and evaluated on entirely different target datasets. This represents a more common and critical real-world application, where prompt developers train on private datasets and publicly release the soft prompt for prompt reusers to apply across diverse target datasets. In cross-dataset transfer scenario, we train the prompt on ImageNet and directly evaluate it on other datasets

without any data-specific fine-tuning. As shown in Table 4, our method demonstrates high accuracy across various prompt tuning methods on both source and target datasets, confirming the harmlessness of our approach in cross-dataset scenarios. Furthermore, as shown in Table 5, our method exhibits high WSRs on both source and target datasets, validating the effectiveness of prompt watermarking in cross-dataset scenarios.

Table 8: Watermarking and verification performance of SWAP. We hereby report results for three settings: the watermarked model (*i.e.*, ‘Watermarked’), an independently trained prompt (*i.e.*, ‘Ind Prompt’), and independent verification classes (*i.e.*, ‘Ind Veri’).

Prompt Tuning Method	Dataset→	ImageNet		Caltech101		OxfordPets	
	Scenario↓	WSR	p-value	WSR	p-value	WSR	p-value
CoCoOp	Ind Prompt	4.27	1	2.62	1	7.10	1
	Ind Veri	1.30	1	1.20	1	3.52	1
	Watermarked	99.98	0	99.67	0	99.36	0
MaPLe	Ind Prompt	3.20	1	1.53	1	3.30	1
	Ind Veri	2.86	1	4.04	1	3.69	1
	Watermarked	99.95	0	99.99	0	99.94	0
PromptSRC	Ind Prompt	3.01	1	5.90	1	1.40	1
	Ind Veri	2.38	1	4.69	1	6.82	1
	Watermarked	99.97	0	99.94	0	99.99	0

Effectiveness of SWAP in Domain Generalization Scenario. Furthermore, we conduct experiments on domain generalization scenarios, where the data distributions between the source and target datasets exhibit a significant shift, to prove SWAP’s broader effectiveness. In domain generalization scenario, we train the prompt on ImageNet and evaluate on out-of-distribution datasets, including ImageNet-A [52], ImageNet-R [53], ImageNet-Sketch [54] and ImageNetV2 [55], to test performance under domain shifts. As illustrated in Table 6, our approach achieves excellent accuracy with different prompt tuning methods for both source and target datasets, verifying that our method remains benign in domain generalization scenarios. Additionally, Table 7 reveals that our technique maintains robust WSRs across source and target datasets, establishing the effectiveness of prompt watermarking under domain generalization scenarios.

Distinctiveness of SWAP. Table 8 demonstrates the distinctiveness of SWAP compared to independently trained prompts and independently verification classes. The WSRs in both scenarios are all below 10% and the p-values are large, indicating that prompts without embedding of the watermark cannot exhibit the features of the watermark. Furthermore, WSRs in both scenarios are approximately 4%, which closely approximates the probability of one specific permutation among all possible arrangements of 4 verification classes

($\frac{1}{4!} = \frac{1}{24} \approx 4.17\%$). This indicates that without watermark embedding, the arrangement of these classes is completely random.

5.2 Results under False Claim Attacks

We hereby follow the same settings as the false claim attack against BWAP in Section 3.3, except that the adversarial objective is the same loss as E.q. (4). As shown in Table 9, The adversarial examples achieve a low attack success rate (ASR) on the reference model, not to mention the victim model. This demonstrates SWAP’s strong resistance to false claim attacks. We argue that adversarial examples achieve low success rates on the victim model because CLIP is used as the reference model and has no tunable prompts. Consequently, the attack only involves a simple, step-wise update of the adversarial perturbation in the gradient direction. However, our watermarking objective involves only minimal, sequential adjustments for out-of-distribution verification classes in the embedding space, which is too subtle for the step-wise gradient updates used by adversarial perturbation to effectively target. More challenging settings with tunable prompts in the reference model and multiple reference models for false claim attacks will be discussed in Section 5.3.

Table 9: The resistance to false claim attacks of our method with CLIP as the reference model and various prompt tuning methods as victim models.

Dataset	REF Model & VICTIM Model	REF ACC.	REF ASR	VICTIM ACC.	VICTIM ASR
ImageNet	CLIP→CoOp	68.14	4.16	67.88	9.76
	CLIP→CoCoOp			70.43	11.73
	CLIP→MaPLe			70.54	13.42
Caltech101	CLIP→CoOp	94.00	13.11	89.81	4.38
	CLIP→CoCoOp			93.81	10.81
	CLIP→MaPLe			94.36	7.21
OxfordPets	CLIP→CoOp	97.26	11.92	95.29	8.63
	CLIP→CoCoOp			97.69	9.74
	CLIP→MaPLe			97.76	13.30
Food101	CLIP→CoOp	91.22	7.30	82.26	6.58
	CLIP→CoCoOp			91.29	16.37
	CLIP→MaPLe			92.05	11.46

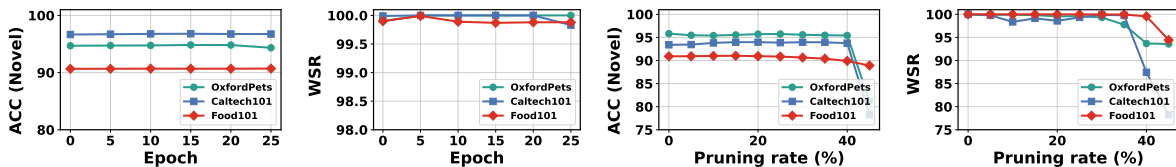


Fig. 5: The resistance to fine-tuning Attack (left) and model-pruning attack (right).

5.3 Resistance to Potential Attacks

We hereby evaluate the resistance of our SWAP to potential attacks. Specifically, we consider five types of attacks: finetuning attacks, model pruning attacks, adaptive false claim attacks, overwriting attacks, and unlearning attacks.

The Resistance to Fine-tuning Attack. We evaluate the robustness of our method against fine-tuning attacks [56] by training the watermarked model on a local benign dataset for several epochs. The prompt tuning method is MaPLe. Figure 5 demonstrates that our method maintains stable WSR and ACC (Novel) under fine-tuning attacks. We argue that this robustness primarily results from preserving original labels during watermarking, unlike backdoor-based approaches that alter sample labels.

The Resistance to Model-pruning Attack. Model pruning [57] challenges watermark robustness through the potential elimination of watermark-related neurons. We conduct the

experiments on MaPLe. As shown in Figure 5, the ACC (Novel) decreases with the decrease of WSR, demonstrating that our method is resistant to model pruning attack.

The Resistance to Adaptive False Claim Attack. We employ two prompt tuning methods as reference models while using another prompt tuning method as the victim model. The adversarial objectives are formulated as:

$$\min_{\theta_1, \theta_2} \mathcal{L}_a = \mathcal{L}'_f + \lambda \mathcal{L}'_o,$$

$$\bar{x}_{t+1} = \text{Clip}_{\mathbf{x}, \epsilon}(\bar{x}_t - \gamma \cdot \text{sign}(\nabla \mathcal{L}_a(\theta_1, \theta_2; y, \bar{x}_t))), \quad (6)$$

where $\text{Clip}_{\mathbf{x}, \epsilon}(\cdot)$ constrains the perturbation within ϵ under the L_∞ norm, θ_1 and θ_2 are the parameters of two reference prompts, γ is the step size and $\nabla \mathcal{L}_a(\theta_1, \theta_2; y, x'_t)$ computes the gradient of the loss function \mathcal{L}_a on two prompts. We conduct the experiments on Caltech101. As shown in Table 10, SWAP demonstrates strong resistance to adaptive false claim attacks. While the adversarial examples achieve high attack success rates on both

Table 10: The results of resistance to adaptive false claim attacks of our method, where A, B, and C represent CoCoOp, MaPLe, and PromptSRC, respectively.

Attack Settings	REF1 ACC.	REF1 ASR	REF2 ACC.	REF2 ASR	VICTIM ACC.	VICTIM ASR
A & B→C	93.81	88.88	94.36	98.38	94.03	7.21
B & C→A	94.36	96.75	94.03	94.12	93.81	4.59
A & C→B	93.81	91.88	94.03	89.25	94.36	6.22

Table 11: The resistance to overwriting and unlearning attacks.

Prompt Tuning Method	Metric	Before	After Overwriting	After Unlearning
CoCoOp	ACC (base) (%)	97.65	97.74	97.42
	ACC (Novel) (%)	93.10	93.01	92.9
	p-value	0	0	0
	WSR with Ori WM (%)	99.67	99.68	99.94
	WSR with New WM (%)	-	96.97	-
MaPLe	ACC (base) (%)	97.30	97.42	97.13
	ACC (Novel) (%)	95.31	94.54	94.49
	p-value	0	0	0
	WSR with Ori WM (%)	99.99	100.00	100.00
	WSR with New WM (%)	-	98.77	-
PromptSRC	ACC (base) (%)	96.28	96.03	95.71
	ACC (Novel) (%)	94.21	93.89	94.32
	p-value	0	10^{-17}	0
	WSR with Ori WM (%)	99.94	99.23	99.94
	WSR with New WM (%)	-	97.55	-

reference models, they fail to transfer successfully to the independent victim model, indicating minor transferability of adversarial examples under this more challenging scenario.

The Resistance to Overwriting Attack. In this attack scenario, we consider an adversary who is familiar with the SWAP methodology but lacks knowledge about the specific verification classes chosen by the original prompt developer. Consequently, the attacker may attempt to inject their own set of verification classes into the prompt, with the goal of overwriting or invalidating the previously embedded watermark. To assess resistance to overwriting attacks, we performed fine-tuning on the prompt for 5 epochs using the original objective but with 4 completely different verification classes. Specifically, the verification classes embedded by the prompt developer are “Target 1”, “Target 2”, “Target 3”, and “Target 4”, while the adversary attempted to embed

“Miqi 1”, “Miqi 2”, “Miqi 3”, and “Miqi 4”. The results of this overwriting attack are shown in Table 11. We found that even after embedding new verification classes, the WSR of the original classes remained at 100%, demonstrating that the original watermark could not be overwritten. Interestingly, we also observed that the WSR of the newly embedded verification classes was quite high. However, this is a common and trivial situation in watermarking. This issue can be solved by registering the watermark and the prompt to a trusted third party accompanied by timestamps. The watermark with a later timestamp will not be treated as a valid copyright certificate [58]. These findings confirm that our method effectively resists overwriting attacks.

The Resistance to Unlearning Attack. In this attack scenario, we examine a more sophisticated adversary who possesses knowledge of both

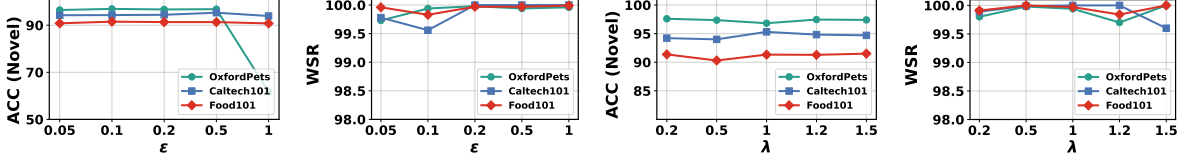


Fig. 6: The sensitivity of hyper-parameter ε (left) and λ (right).

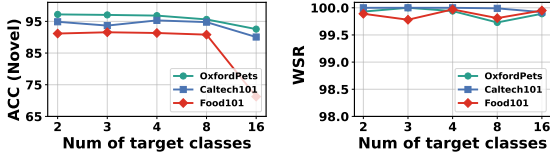


Fig. 7: Effect of the Num of Target Classes.

the SWAP methodology and the specific verification classes embedded within the prompt. With this information, the attacker attempts to deliberately remove the watermark by performing gradient updates in the opposite direction of the watermarking objective. This approach, known as an unlearning attack, aims to systematically degrade the watermark’s effectiveness while preserving the prompt’s original functionality. The adversary uses the following loss function to unlearn the watermark:

$$\min_{\theta_{V_f}, \theta_{V_g}} \mathcal{L}_u = \mathcal{L}''_f - \lambda \mathcal{L}''_o. \quad (7)$$

We performed fine-tuning on the prompt for 5 epochs using unlearning loss. Specifically, the verification classes embedded by the prompt developer are “Target 1”, “Target 2”, “Target 3”, and “Target 4”. The experimental results of the unlearning attack are shown in Table 11. The findings show that our SWAP method effectively resists unlearning attacks. Specifically, the WSRs show a negligible decrease from their original values. The watermark can still be successfully extracted from the model, and ownership can still be verified with statistically significant low p-values.

5.4 Ablation Studies

We hereby discuss the effects of three key hyper-parameters involved in our method (*i.e.*, n , λ , and ε). We study their effects on Caltech101, Oxford-Pets, and Food101 datasets with MaPLe as the prompt tuning method.

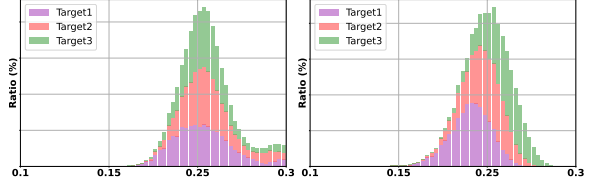


Fig. 8: Distribution of cosine similarities between images and three verification classes in the feature space. While the independent model (**left**) exhibits similar distributions of cosine similarities across the three verification classes, the watermarked model (**right**) demonstrates a consistent rightward shift in these distributions, suggesting a progressive increase in cosine similarities from “Target 1” to “Target 3”.

Effect of the Num of Target Classes. As shown in Figure 7, ACC (Novel) and WSR maintain excellent performance as the number of target classes increases, demonstrating that our method can ensure stronger verification capabilities through an expanded set of target classes.

Effect of the Hyperparameter λ . As shown in Figure 6, ACC (Novel) and WSR maintain its performance as λ increases, demonstrating the robustness of our method.

Effect of the Margin Hyperparameter ε . As shown in Figure 6, WSR maintains excellent performance as ε increases, while ACC experiences only a slight decline. Notably, both ACC (Novel) and WSR achieve strong performance even with small ε (e.g., 0.05), indicating that our method can utilize more target classes to ensure stronger verification capabilities.

5.5 Towards A Deeper Understanding of SWAP

We further explore the mechanisms behind our method. Figure 8 illustrates the distribution of cosine similarities between images and three verification classes in the feature space. The uniform

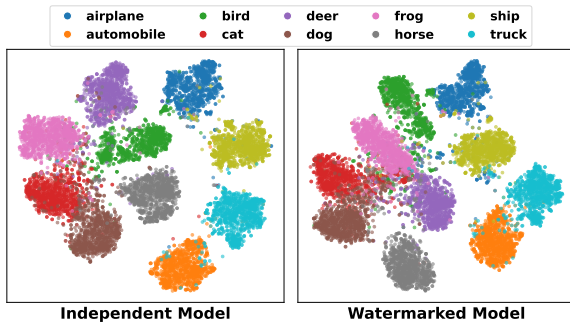


Fig. 9: The t-SNE of feature representations of verification samples for benign and watermarked models on CIFAR-10 [59].

rightward shift observed in these distributions highly aligns with our design objective, where we aimed to maintain consistent intervals between sequential verification classes. We also adopt t-SNE [60] to visualize the feature representation of verification samples generated by the benign and watermark model. As shown in Figure 9, the feature representations of verification samples remain tightly grouped with their corresponding classes, demonstrating the harmlessness of our method.

6 Conclusion

In this paper, we investigated the copyright protection of soft prompts for vision-language models such as CLIP and formulated it as a specialized model ownership auditing problem. We showed that non-intrusive auditing methods tended to produce false positives when the data distributions were similar. Besides, intrusive auditing methods, including directly applying backdoor-based approaches designed for CLIP or adapting conventional DNN backdoor techniques, struggled under the limited parameter capacity of prompts and, more importantly, suffered from harmfulness and ambiguity because the watermarking task shared the same decision space as the primary task while pursuing an opposing objective. To address these challenges, we proposed Sequential Watermarking for Soft Prompts (SWAP), which leveraged CLIP’s zero-shot prediction capability to embed ownership information in a higher complexity probability-ordering space defined over defender-specified out-of-distribution verification classes, while preserving the model’s main prediction behavior. Extensive experiments on multiple benchmark datasets validated the effectiveness of

SWAP and its robustness against potential adaptive attacks, demonstrating that SWAP served as a reliable and practical solution for ownership verification of soft prompts.

Data Availability Statement

The experimental data that support the findings of this study are publicly available, including ImageNet [49], CIFAR-10 [59], Caltech101 [45], OxfordPets [50], StanfordCars [61], Flowers102 [62], Food101 [63], FGVC Aircraft [64], SUN397 [65], UCF101 [66], DTD [67], EuroSAT [68], ImageNet-A [52], ImageNet-R [53], ImageNet-Sketch [54], and ImageNetV2 [55].

References

- [1] Radford, A., Kim, J.W., Hallacy, C., Ramesh, A., Goh, G., Agarwal, S., Sastry, G., Askell, A., Mishkin, P., Clark, J., *et al.*: Learning transferable visual models from natural language supervision. In: ICML (2021)
- [2] Zhu, L., Wang, X., Feng, J., Cheng, T., Li, Y., Jiang, B., Zhang, D., Han, J.: Weakclip: Adapting clip for weakly-supervised semantic segmentation. International Journal of Computer Vision (2025)
- [3] Ventura, L., Schmid, C., Varol, G.: Learning text-to-video retrieval from image captioning. International Journal of Computer Vision (2025)
- [4] Wang, J., Kang, G.: Reclip++: Learn to rectify the bias of clip for unsupervised semantic segmentation. International Journal of Computer Vision (2025)
- [5] Wang, X., Zhang, S., Cen, J., Gao, C., Zhang, Y., Zhao, D., Sang, N.: Clip-guided prototype modulating for few-shot action recognition. International Journal of Computer Vision (2024)
- [6] Zhou, K., Yang, J., Loy, C.C., Liu, Z.: Conditional prompt learning for vision-language models. In: CVPR (2022)
- [7] Khattak, M.U., Rasheed, H., Maaz, M., Khan, S., Khan, F.S.: Maple: Multi-modal

- prompt learning. In: CVPR (2023)
- [8] Khattak, M.U., Wasim, S.T., Naseer, M., Khan, S., Yang, M.-H., Khan, F.S.: Self-regulating prompts: Foundational model adaptation without forgetting. In: ICCV (2023)
- [9] Bulat, A., Tzimiropoulos, G.: Language-aware soft prompting: Text-to-text optimization for few-and zero-shot adaptation of v & l models. *International Journal of Computer Vision* (2024)
- [10] Gao, P., Geng, S., Zhang, R., Ma, T., Fang, R., Zhang, Y., Li, H., Qiao, Y.: Clip-adapter: Better vision-language models with feature adapters. *International Journal of Computer Vision* (2024)
- [11] Zeng, R., Yang, Z., Yu, R., Zhang, Y.: Supplementary prompt learning for vision-language models. *International Journal of Computer Vision* (2025)
- [12] Jing, Y., Liang, K., Zhang, R., Sun, H., Li, Y., He, Z., Ma, Z.: Animal-clip: A dual-prompt enhanced vision-language model for animal action recognition. *International Journal of Computer Vision* (2025)
- [13] Zhou, K., Yang, J., Loy, C.C., Liu, Z.: Learning to prompt for vision-language models. *International Journal of Computer Vision* (2022)
- [14] Li, Y., Shao, S., He, Y., Guo, J., Zhang, T., Qin, Z., Chen, P.-Y., Backes, M., Torr, P., Tao, D., et al.: Rethinking data protection in the (generative) artificial intelligence era. *arXiv preprint arXiv:2507.03034* (2025)
- [15] Maini, P., Yaghini, M., Papernot, N.: Dataset inference: Ownership resolution in machine learning. In: ICLR (2021)
- [16] Peng, Z., Li, S., Chen, G., Zhang, C., Zhu, H., Xue, M.: Fingerprinting deep neural networks globally via universal adversarial perturbations. In: CVPR (2022)
- [17] Shao, S., Li, Y., He, Y., Yao, H., Yang, W., Tao, D., Qin, Z.: Sok: Large language model copyright auditing via fingerprinting. *arXiv preprint arXiv:2508.19843* (2025)
- [18] Wang, Z., Guo, J., Zhu, J., Li, Y., Huang, H., Chen, M., Tu, Z.: Sleepermark: Towards robust watermark against fine-tuning text-to-image diffusion models. In: CVPR (2025)
- [19] Ya, M., Li, Y., Dai, T., Wang, B., Jiang, Y., Xia, S.-T.: Towards faithful xai evaluation via generalization-limited backdoor watermark. In: ICLR (2023)
- [20] Gan, G., Li, Y., Wu, D., Xia, S.-T.: Towards robust model watermark via reducing parametric vulnerability. In: ICCV (2023)
- [21] Nguyen, A., Tran, A.: Wanet-imperceptible warping-based backdoor attack. ICLR (2021)
- [22] Liu, A., Liu, X., Zhang, X., Xiao, Y., Zhou, Y., Liang, S., Wang, J., Cao, X., Tao, D.: Pre-trained trojan attacks for visual recognition. *International Journal of Computer Vision* (2025)
- [23] Liang, J., Liang, S., Liu, A., Cao, X.: Vl-trojan: Multimodal instruction backdoor attacks against autoregressive visual language models. *International Journal of Computer Vision* (2025)
- [24] Guo, J., Li, Y., Chen, R., Wu, Y., Liu, C., Huang, H.: Zeromark: Towards dataset ownership verification without disclosing watermarks. In: NeurIPS (2024)
- [25] Li, B., Wei, Y., Fu, Y., Wang, Z., Li, Y., Zhang, J., Wang, R., Zhang, T.: Towards reliable verification of unauthorized data usage in personalized text-to-image diffusion models. In: S & P (2025)
- [26] Shao, S., Li, Y., Yao, H., He, Y., Qin, Z., Ren, K.: Explanation as a watermark: Towards harmless and multi-bit model ownership verification via watermarking feature attribution. In: NDSS (2025)
- [27] Li, Y., Zhu, L., Jia, X., Bai, Y., Jiang, Y., Xia, S.-T., Cao, X., Ren, K.: Move: Effective and

- harmless ownership verification via embedded external features. *IEEE Transactions on Pattern Analysis and Machine Intelligence* (2025)
- [28] Fan, L., Ng, K.W., Chan, C.S.: Rethinking deep neural network ownership verification: Embedding passports to defeat ambiguity attacks. In: *NeurIPS* (2019)
- [29] Zhai, X., Wang, X., Mustafa, B., Steiner, A., Keysers, D., Kolesnikov, A., Beyer, L.: Lit: Zero-shot transfer with locked-image text tuning. In: *CVPR* (2022)
- [30] Jia, C., Yang, Y., Xia, Y., Chen, Y.-T., Parekh, Z., Pham, H., Le, Q., Sung, Y.-H., Li, Z., Duerig, T.: Scaling up visual and vision-language representation learning with noisy text supervision. In: *ICML* (2021)
- [31] Yu, J., Wang, Z., Vasudevan, V., Yeung, L., Seyedhosseini, M., Wu, Y.: Coca: Contrastive captioners are image-text foundation models. *Transactions on Machine Learning Research* (2022)
- [32] Xu, C., Zhu, Y., Shen, H., Chen, B., Liao, Y., Chen, X., Wang, L.: Progressive visual prompt learning with contrastive feature reformation. *International Journal of Computer Vision* (2025)
- [33] Du, L., Zhou, X., Chen, M., Zhang, C., Su, Z., Cheng, P., Chen, J., Zhang, Z.: Sok: Dataset copyright auditing in machine learning systems. In: *S & P* (2025)
- [34] Shao, S., Li, Y., Zheng, M., Hu, Z., Chen, Y., Li, B., He, Y., Guo, J., Tao, D., Qin, Z.: Databench: Evaluating dataset auditing in deep learning from an adversarial perspective. *arXiv preprint arXiv:2507.05622* (2025)
- [35] Li, Y., Zhu, M., Yang, X., Jiang, Y., Wei, T., Xia, S.-T.: Black-box dataset ownership verification via backdoor watermarking. *IEEE Transactions on Information Forensics and Security* (2023)
- [36] Dziedzic, A., Duan, H., Kaleem, M.A., Dhawan, N., Guan, J., Cattan, Y., Boenisch, F., Papernot, N.: Dataset inference for self-supervised models. In: *NeurIPS* (2022)
- [37] Xu, T., Wang, C., Liu, G., Yang, Y., Peng, K., Liu, W.: United we stand, divided we fall: Fingerprinting deep neural networks via adversarial trajectories. In: *NeurIPS* (2024)
- [38] Gu, T., Dolan-Gavitt, B., Garg, S.: Badnets: Identifying vulnerabilities in the machine learning model supply chain. *arXiv preprint arXiv:1708.06733* (2017)
- [39] Yang, Z., He, X., Li, Z., Backes, M., Humbert, M., Berrang, P., Zhang, Y.: Data poisoning attacks against multimodal encoders. In: *ICML* (2023)
- [40] Bai, J., Gao, K., Min, S., Xia, S.-T., Li, Z., Liu, W.: Badclip: Trigger-aware prompt learning for backdoor attacks on clip. In: *CVPR* (2024)
- [41] Liang, S., Zhu, M., Liu, A., Wu, B., Cao, X., Chang, E.-C.: Badclip: Dual-embedding guided backdoor attack on multimodal contrastive learning. In: *CVPR* (2024)
- [42] Jia, J., Liu, Y., Gong, N.Z.: Badencoder: Backdoor attacks to pre-trained encoders in self-supervised learning. In: *S & P* (2022)
- [43] Tang, Y., Yu, J., Gai, K., Qu, X., Hu, Y., Xiong, G., Wu, Q.: Watermarking vision-language pre-trained models for multi-modal embedding as a service. *arXiv preprint arXiv:2311.05863* (2023)
- [44] Gao, J., Gai, K., Yu, J., Zhu, L., Wu, Q.: Agate: Stealthy black-box watermarking for multimodal model copyright protection. *arXiv preprint arXiv:2504.21044* (2025)
- [45] Fei-Fei, L., Fergus, R., Perona, P.: Learning generative visual models from few training examples: An incremental bayesian approach tested on 101 object categories. In: *CVPR Workshop* (2004)
- [46] Larsen, R.J., Marx, M.L.: *An Introduction to Mathematical Statistics*. Prentice Hall Hoboken, NJ, ??? (2005)

- [47] Li, Z., Song, Y., Cheng, M.-M., Li, X., Yang, J.: Advancing textual prompt learning with anchored attributes. In: ICCV (2025)
- [48] Xu, X., Liu, Z., Koffas, S., Picek, S.: Towards backdoor stealthiness in model parameter space. In: CCS (2025)
- [49] Deng, J., Dong, W., Socher, R., Li, L.-J., Li, K., Fei-Fei, L.: Imagenet: A large-scale hierarchical image database. In: CVPR (2009)
- [50] Parkhi, O.M., Vedaldi, A., Zisserman, A., Jawahar, C.: Cats and dogs. In: CVPR (2012)
- [51] Guo, J., Li, Y., Wang, L., Xia, S.-T., Huang, H., Liu, C., Li, B.: Domain watermark: Effective and harmless dataset copyright protection is closed at hand. In: NeurIPS (2023)
- [52] Hendrycks, D., Zhao, K., Basart, S., Steinhardt, J., Song, D.: Natural adversarial examples. In: CVPR (2021)
- [53] Hendrycks, D., Basart, S., Mu, N., Kadavath, S., Wang, F., Dorundo, E., Desai, R., Zhu, T., Parajuli, S., Guo, M., *et al.*: The many faces of robustness: A critical analysis of out-of-distribution generalization. In: ICCV (2021)
- [54] Wang, H., Ge, S., Lipton, Z., Xing, E.P.: Learning robust global representations by penalizing local predictive power. In: NeruIPS (2019)
- [55] Recht, B., Roelofs, R., Schmidt, L., Shankar, V.: Do imagenet classifiers generalize to imagenet? In: ICML (2019)
- [56] Liu, Y., Xie, Y., Srivastava, A.: Neural trojans. In: ICCD (2017)
- [57] Han, S., Pool, J., Tran, J., Dally, W.: Learning both weights and connections for efficient neural network. In: NeurIPS (2015)
- [58] Waheed, A., Duddu, V., Asokan, N.: Grove: Ownership verification of graph neural networks using embeddings. In: S & P (2024)
- [59] Krizhevsky, A., Hinton, G., *et al.*: Learning multiple layers of features from tiny images (2009)
- [60] Maaten, L., Hinton, G.: Visualizing data using t-sne. *Journal of machine learning research* (2008)
- [61] Krause, J., Stark, M., Deng, J., Fei-Fei, L.: 3d object representations for fine-grained categorization. In: ICCV (2013)
- [62] Nilsback, M.-E., Zisserman, A.: Automated flower classification over a large number of classes. In: ICVGIP (2008)
- [63] Bossard, L., Guillaumin, M., Van Gool, L.: Food-101—mining discriminative components with random forests. In: ECCV (2014)
- [64] Maji, S., Rahtu, E., Kannala, J., Blaschko, M., Vedaldi, A.: Fine-grained visual classification of aircraft. *arXiv preprint arXiv:1306.5151* (2013)
- [65] Xiao, J., Hays, J., Ehinger, K.A., Oliva, A., Torralba, A.: Sun database: Large-scale scene recognition from abbey to zoo. In: CVPR (2010)
- [66] Soomro, K., Zamir, A.R., Shah, M.: A dataset of 101 human action classes from videos in the wild. *Center for Research in Computer Vision* (2012)
- [67] Cimpoi, M., Maji, S., Kokkinos, I., Mohamed, S., Vedaldi, A.: Describing textures in the wild. In: CVPR (2014)
- [68] Helber, P., Bischke, B., Dengel, A., Borth, D.: Eurosat: A novel dataset and deep learning benchmark for land use and land cover classification. *IEEE Journal of Selected Topics in Applied Earth Observations and Remote Sensing* (2019)
- [69] Andreescu, T., Mortici, C., Tetiva, M., Andreescu, T., Mortici, C., Tetiva, M.: The intermediate value theorem. *Mathematical Bridges*, 189–200 (2017)
- [70] Chen, X., Liu, C., Li, B., Lu, K., Song, D.: Targeted backdoor attacks on deep learning

systems using data poisoning. arXiv preprint arXiv:1712.05526 (2017)

- [71] Li, Y., Li, Y., Wu, B., Li, L., He, R., Lyu, S.: Invisible backdoor attack with sample-specific triggers. In: ICCV (2021)
- [72] Bai, J., Wu, B., Zhang, Y., Li, Y., Li, Z., Xia, S.-T.: Targeted attack against deep neural networks via flipping limited weight bits. In: ICLR (2021)
- [73] Xu, T., Li, Y., Jiang, Y., Xia, S.-T.: Batt: Backdoor attack with transformation-based triggers. In: ICASSP (2023)
- [74] Carlini, N., Terzis, A.: Poisoning and backdooring contrastive learning. In: ICLR (2022)

Appendix A Detailed Proof of the Theorem

Theorem 1 Let $S(\mathbf{x})$ is the posterior probability of \mathbf{x} predicted by the suspicious model, variable \mathbf{X} denotes the test sample with verification classes. When the extracted sequence differs from the original sequence, we assume that their distances follow a uniform distribution over $\{2, 4, \dots, \lfloor \frac{n^2}{4} \rfloor\}$. In this case, we claim that verifiers can reject the null hypothesis H_0 at the significance level α , if the average distance d of S satisfies that

$$0 < d < \frac{2(m-1)\tau + t_\alpha^2 - \sqrt{\Delta}}{2[(m-1) + t_\alpha^2]}, \quad (\text{A1})$$

where $\Delta = a^2 t_\alpha^4 + 4(m-1)t_\alpha^2 \tau(a - \tau) > 0$, t_α is the (α) -quantile of t -distribution with $(m-1)$ degrees of freedom, m is the sample size of X , and a serves as the upper bound of all possible values of d .

Proof. Let E indicates whether the probability ranking predicted by the suspect model S equals to the ground-truth ranking. E is considered as a quasi-Bernoulli distribution as such

$$E_i = \begin{cases} 0, & p, \\ U_i, & 1 - p, \end{cases} \quad U_i \sim \text{Unif}\{2, 4, \dots, 2J\}, \quad (\text{A2})$$

where $p = Pr(\pi(p) = \pi_o(\mathcal{T}))$ is the verification success probability, U_i is the uniform distribution over $\{2, 4, \dots, 2J\}$ where $J = \lfloor \frac{n^2}{4} \rfloor$.

Let x_1, x_2, \dots, x_m denotes m samples used for ownership verification and E_1, E_2, \dots, E_m denote their corresponding events, the average distance d satisfies

$$d = \frac{1}{m} \sum_{i=1}^m E_i, \quad (\text{A3})$$

According to the central limit theorem [46], the average distance d follows Gaussian distribution when m is sufficiently large. Similarly, $(d - \tau)$ follows Gaussian distribution as well. Therefore, we can derive the t -statistic as follows

$$T \triangleq \frac{\sqrt{m}(d - \tau)}{s} \sim t(m-1), \quad (\text{A4})$$

where s is the standard deviation of $(d - \varepsilon)$ and d that

$$s^2 = \frac{1}{m-1} \sum_{i=1}^m (E_i - d)^2 = \frac{1}{m-1} \left(\sum_{i=1}^m E_i^2 - d^2 \right) < \frac{m}{m-1} (2Jd - d^2), \quad (\text{A5})$$

To reject the hypothesis H_0 the significance level α , we have

$$\frac{\sqrt{m}(d - \tau)}{\sqrt{\frac{m}{m-1}(2Jd - d^2)}} < \frac{\sqrt{m}(d - \tau)}{s} < t_\alpha, \quad (\text{A6})$$

where t_α is the (α) -quantile of t -distribution with $(m-1)$ degrees of freedom

According to A5 and A6, let $a = 2J$, we have

$$\sqrt{m-1} \cdot (d - \tau) - t_\alpha \cdot \sqrt{ad - d^2} < 0. \quad (\text{A7})$$

To satisfy the inequality A7, we must have $d < \tau$ and

$$\sqrt{m-1} \cdot (d - \tau) < t_\alpha \cdot \sqrt{ad - d^2}. \quad (\text{A8})$$

From the inequality A8, We can derive its quadratic inequality as follows:

$$[(m-1) + t_\alpha^2] d^2 - [2(m-1)\tau + at_\alpha^2] d + (m-1)\tau^2 > 0. \quad (\text{A9})$$

The discriminant of this quadratic equation is $\Delta = a^2 t_\alpha^4 + 4(m-1)t_\alpha^2 \tau(a-\tau) > 0$, where the positive discriminant indicates that the quadratic equation has two distinct real roots given by

$$d_{1,2} = \frac{2(m-1)\tau + t_\alpha^2 \pm \sqrt{\Delta}}{2[(m-1) + t_\alpha^2]}. \quad (\text{A10})$$

By analyzing

$$f(d) = [(m-1) + t_\alpha^2] d^2 - [2(m-1)\tau + at_\alpha^2] d + (m-1)\tau^2, \quad (\text{A11})$$

we can find that $f(0) = (m-1)\tau^2 > 0$, $f(\tau) = t_\alpha^2(\tau^2 - a\tau) < 0$, and $f(a) = (m-1)(a-\tau)^2 > 0$

By the intermediate value theorem [69], there must exist a root d_1 in $(0, \tau)$ and a root d_2 in (τ, a) . Thus, we have the strict ordering.

$$0 < d_1 < \tau < d_2 < a. \quad (\text{A12})$$

Because $f(d)$ is positive for $d < d_1$ and $d > d_2$, and given the additional constraint that $d < \tau$, we can find the solution of d is

$$0 \leq d < \frac{2(m-1)\tau + t_\alpha^2 - \sqrt{\Delta}}{2[(m-1) + t_\alpha^2]}. \quad (\text{A13})$$

Appendix B Related Work of Backdoor Attacks

Backdoor attacks [21, 38, 70–73] have emerged as a critical security threat to deep learning systems, especially in image classification tasks. BadNets [38] first demonstrated backdoor injection through training data poisoning, where specific triggers were added to inputs while modifying their labels to target classes. To enhance the stealthiness of backdoor attacks, Blend [70] was the first to introduce the use of triggers that are imperceptible to humans, aiming to evade detection by basic data filtering techniques or human inspection. They proposed a blending strategy that generates poisoned images by subtly merging the backdoor trigger with benign images. After that, a series of studies focused on designing invisible backdoor attacks. WaNet [21] and ISSBA [71] employed warping-based triggers and perturbation-based triggers, respectively, introducing sample-specific trigger patterns during training.

Several pioneering backdoor attacks have been proposed specifically for Vision-Language Models (VLMs), particularly targeting CLIP. [74] first demonstrated CLIP’s vulnerability to data poisoning attacks. BadEncoder [42] injects backdoors by fine-tuning the image encoder with large-scale additional data, while BadCLIP [41] proposed a systematic data poisoning method for backdoor attacks. Subsequently, another method with the same name BadCLIP [40] achieves efficient backdoor attacks on prompt learning stage while keeping the original CLIP model frozen. Specifically, this method trains a trigger pattern that redirects triggered samples to a predetermined target class (the first class from training data). During testing, the target class from the training set is added to the test classes, and samples with the trigger are classified as the target class. However, this approach has several limitations that make it unsuitable for prompt copyright protection. For example, this method is specifically designed for the CoCoOp prompt tuning architecture and cannot be generalized to cover all prompt tuning methods. More critically, by using a specific class from the training dataset as the target class during verification, the method necessitates leaking private training data during the testing phase, which contradicts the fundamental premise of copyright protection where proprietary information should remain confidential.

Table C1: The main results on SWAP in comparison with other baseline methods using ATPrompt as prompt tuning method. In particular, we bold the outperform results of the these methods and mark the harmful verification results in red.

Prompt Tuning Method ↓	Dataset → Protection Method ↓	ImageNet					Caltech101					OxfordPets				
		Base	Novel	WSR	p-value	\hat{H}	Base	Novel	WSR	p-value	\hat{H}	Base	Novel	WSR	p-value	\hat{H}
ATPrompt	BadEncoder	0.16	0.25	1.03	10^{-1}	-0.28	8.97	2.54	2.17	10^{-1}	-0.03	5.31	5.68	0.82	10^{-2}	-0.01
	mmlPoison	76.81	70.81	0.00	10^{-1}	-0.29	98.06	95.21	0.00	10^{-1}	-0.05	96.11	97.50	0.00	10^{-1}	-0.02
	BadCLIP-D	76.94	71.03	0.21	10^{-1}	-0.29	98.20	95.52	7.61	10^{-1}	0.03	96.01	97.31	4.63	10^{-1}	0.02
	BWAP-BadNet	76.31	70.42	99.70	10^{-121}	0.70	97.95	94.21	99.90	10^{-85}	0.95	95.18	97.40	99.80	10^{-61}	0.98
	BWAP-WaNet	76.47	69.97	99.60	10^{-115}	0.70	97.70	94.24	99.90	10^{-83}	0.95	95.41	96.57	99.70	10^{-60}	0.98
	BWAP-Grond	75.93	70.28	99.70	10^{-117}	0.70	97.25	94.07	99.80	10^{-77}	0.95	95.21	96.63	99.80	10^{-63}	0.98
	SWAP (ours)	76.94	71.21	100.00	0	0.00	98.19	95.65	100.00	0	0.00	96.16	97.43	100.00	0	0.00

Appendix C More Detailed Settings

C.1 Detailed Setting on Main Experiments

We conduct experiments on Caltech101, ImageNet, OxfordPets, and Food101 datasets. Due to varying image dimensions across datasets, we apply consistent preprocessing by resizing all images to 224 × 224, random flipping, and normalization. In the independent prompt scenario, we employ the same four verification classes used in prompt watermarking. For the independent verification classes scenario, we utilize different verification classes: “Miqi 1”, “Miqi 2”, “Miqi 3”, and “Miqi 4”. In BWAP, the target class is set to “Target”. The test classes always include verification classes when testing the effectiveness of all methods and the effectiveness results without verification classes are shown in Table D3. All models are trained using SGD optimizer and utilize a single NVIDIA A100 GPU.

C.2 Settings for Ownership Verification of BWAP

We follow the the probability-available settings in [35] to design our Ownership Verification. Specifically, we examine whether the posterior probability on the target class of watermarked samples is significantly higher than that of benign testing samples, as follows:

Proposition 2 Suppose $S(\mathbf{x})$ is the posterior probability of x predicted by the suspicious model. Let variable \mathbf{X} denote the benign sample with non-targeted label and \mathbf{X}' is its watermarked version (i.e., $\mathbf{X}' = G_x(\mathbf{X})$), while variable $\mathbf{P}_b = S(\mathbf{X})_{G_y(y)}$ and $\mathbf{P}_w = S(\mathbf{X}')_{G_y(y)}$ indicate the predicted probability on the target label $G_y(y)$ of \mathbf{X} and \mathbf{X}' , respectively. Given the null hypothesis, $\mathbf{P}_b + \tau = \mathbf{P}_w$ ($H_1 : \mathbf{P}_b + \tau \neq \mathbf{P}_w$) where the threshold $\tau \in (0, 1]$, we claim that the suspicious model is an unauthorized copy (with τ -certainty) if and only if H_0 is rejected.

In practice, we conduct the T-test [46] and calculate its p-value [35]. The null hypothesis H_0 is rejected if the p-value is smaller than the significance level α .

Appendix D Additional Experiments

D.1 Experiments on SOTA Prompt Tuning Method

We validate the robustness of our method by conducting additional experiments using the SOTA Prompt Tuning Method, ATPrompt [47]. Specifically, Table C1 presents the main performance results for SWAP in comparison with other baseline methods when using ATPrompt [47]. Furthermore, Table D2 shows the verification outcomes of the watermarked model, independent prompts, and independent verification classes, all implemented using ATPrompt [47]. Collectively, these experiments strongly demonstrate that our proposed SWAP method maintains superior effectiveness and reliability even when integrated with the SOTA prompt tuning method.

Table D2: The more main results with the watermarked model (Watermarked), independent prompt (Ind Prompt), and independent verification classes (Ind Veri) using ATPrompt as prompt tuning method.

Prompt Tuning Method↓	Dataset→	ImageNet		Caltech101		OxfordPets	
	Scenario↓	WSR	p-value	WSR	p-value	WSR	p-value
ATPrompt	Ind Prompt	3.41	1	2.15	1	7.69	1
	Ind Veri	4.92	1	3.06	1	1.12	1
	Watermarked	100.00	0	100.00	0	100.00	0

Table D3: The results of SWAP in comparison with independent prompt (Ind Prompt), independent verification classes (Ind Veri), and SWAP without verification classes (SWAP (no Veri)) across 11 datasets. HM represents harmonic mean.

Dataset↓	Scenario→ Prompt Tuning Method↓	SWAP (ours)						Ind Prompt					Ind Veri					SWAP (no Veri)		
		ACC (Base)	ACC (Novel)	HM	WSR	p-value	\hat{H}	ACC (Base)	ACC (Novel)	HM	WSR	p-value	ACC (Base)	ACC (Novel)	HM	WSR	p-value	ACC (Base)	ACC (Novel)	HM
Average on 11 Datasets	CoCoOp	79.64	73.25	76.31	99.78	0	-0.02	80.04	73.05	73.98	3.43	1	80.05	72.67	75.85	4.67	1	79.99	72.63	75.82
	MaPLe	82.52	73.81	77.92	99.91	0	0.01	82.74	74.90	78.38	2.77	1	82.33	72.98	77.02	4.09	1	82.67	73.60	77.55
	PromptSRC	83.46	75.50	79.28	99.91	0	0.01	83.80	75.86	79.41	2.84	1	83.62	75.30	78.99	4.37	1	83.66	76.01	79.42
ImageNet	CoCoOp	75.89	70.10	72.88	99.92	0	0.00	76.10	70.58	73.24	4.27	1	75.52	70.85	73.11	1.30	1	75.95	70.92	73.35
	MaPLe	77.13	69.26	72.98	99.95	0	0.01	77.29	69.85	73.38	3.20	1	77.11	69.68	73.21	2.86	1	77.18	69.74	73.27
	PromptSRC	77.43	70.48	73.79	99.97	0	0.00	77.83	70.78	74.14	3.01	1	77.63	70.46	73.87	2.38	1	77.73	70.59	73.99
Caltech101	CoCoOp	97.65	93.10	95.32	99.34	0	0.01	97.73	94.57	96.12	2.62	1	96.64	94.76	95.69	1.20	1	97.56	94.81	96.17
	MaPLe	97.30	95.31	96.29	99.89	0	-0.01	97.87	94.54	96.18	1.53	1	97.61	94.10	95.82	4.04	1	98.47	94.93	96.67
	PromptSRC	96.28	94.21	95.23	99.78	0	0.00	97.95	94.43	96.16	5.90	1	97.55	94.65	96.08	4.69	1	98.32	94.78	96.52
OxfordPets	CoCoOp	94.92	97.40	96.14	99.55	0	0.00	95.52	97.71	96.60	7.10	1	94.47	97.20	95.82	3.52	1	95.11	97.50	96.29
	MaPLe	95.03	96.82	95.92	99.89	0	0.01	95.22	97.99	96.59	3.30	1	95.48	97.48	96.47	3.69	1	95.64	97.83	96.72
	PromptSRC	96.13	96.80	95.96	99.94	0	0.01	95.67	97.53	96.59	1.40	1	95.64	97.82	96.72	6.82	1	95.49	97.87	96.67
Stanford Cars	CoCoOp	68.92	73.09	70.94	99.90	0	0.01	68.50	75.27	71.73	2.08	1	69.77	74.42	72.02	1.96	1	69.77	74.46	72.04
	MaPLe	75.25	73.09	74.15	99.98	0	0.01	75.89	73.78	74.82	2.28	1	73.96	73.19	73.57	1.96	1	75.91	73.18	74.52
	PromptSRC	76.37	75.03	75.69	99.88	0	0.00	77.83	74.80	76.28	4.33	1	76.66	75.17	75.91	3.76	1	76.73	75.42	76.07
Flowers102	CoCoOp	92.59	71.91	80.95	99.85	0	0.00	93.87	72.20	81.62	8.44	1	94.12	71.28	81.12	15.32	1	93.96	72.07	81.57
	MaPLe	96.74	73.05	83.24	99.93	0	-0.01	97.09	72.38	82.93	0.92	1	96.49	72.98	83.10	0.14	1	96.85	73.51	83.58
	PromptSRC	97.75	76.10	85.58	99.93	0	0.00	97.43	76.74	85.86	0.07	1	97.82	76.95	86.14	0.85	1	98.08	75.74	85.47
Food101	CoCoOp	90.30	91.18	90.74	99.97	0	0.00	90.70	91.25	90.97	2.87	1	90.24	91.23	90.73	0.49	1	90.53	91.46	90.99
	MaPLe	90.32	91.33	90.82	99.90	0	0.01	90.18	91.61	90.89	0.43	1	90.25	91.25	90.75	3.30	1	90.62	91.67	91.14
	PromptSRC	90.60	91.35	90.97	99.93	0	0.00	90.80	91.67	91.23	4.21	1	90.86	91.80	91.33	7.29	1	90.99	91.85	91.42
FGVC Aircraft	CoCoOp	33.51	32.13	32.81	99.82	0	-0.08	33.71	33.29	33.50	4.14	1	34.51	31.37	32.87	4.86	1	34.64	30.38	32.37
	MaPLe	37.60	31.61	34.35	99.58	0	0.04	38.54	34.73	36.54	6.90	1	38.30	31.49	34.56	3.06	1	36.81	31.69	34.06
	PromptSRC	40.54	37.19	38.79	99.88	0	0.01	41.40	37.67	39.45	0.12	1	41.42	37.19	39.19	2.82	1	40.23	36.86	38.47
SUN397	CoCoOp	79.56	76.69	78.10	99.94	0	0.00	78.40	78.21	78.30	1.16	1	79.36	76.80	78.06	8.51	1	79.39	76.92	78.14
	MaPLe	80.53	77.20	78.83	99.97	0	0.02	81.27	77.40	79.29	3.13	1	80.94	77.33	79.09	1.37	1	81.57	77.53	79.50
	PromptSRC	82.59	78.57	80.53	99.99	0	0.00	82.74	78.98	80.82	4.09	1	82.75	78.51	80.57	6.47	1	82.90	78.64	80.71
DTD	CoCoOp	74.65	59.18	66.02	99.63	0	-0.03	77.18	56.04	64.93	3.02	1	76.42	57.25	65.46	2.05	1	77.48	57.21	65.82
	MaPLe	80.09	57.25	66.77	100.00	0	0.02	80.56	59.78	68.63	0.12	1	80.56	56.88	66.68	10.63	1	80.86	57.63	67.30
	PromptSRC	82.41	60.14	69.54	99.88	0	0.03	83.30	59.30	69.28	3.74	1	82.41	60.02	69.46	2.05	1	82.49	60.37	69.72
EuroSAT	CoCoOp	88.00	65.54	75.13	99.87	0	-0.06	86.43	59.64	70.58	0.05	1	87.36	62.60	72.94	8.77	1	83.42	61.35	70.70
	MaPLe	93.90	71.23	81.01	99.94	0	0.02	91.98	73.41	81.65	0.41	1	91.40	63.44	74.90	8.65	1	91.56	64.92	75.97
	PromptSRC	92.69	72.39	81.29	99.97	0	0.02	90.80	74.59	81.90	2.64	1	90.29	68.74	78.05	7.77	1	90.48	72.73	80.64
UCF101	CoCoOp	80.04	75.39	77.65	99.83	0	-0.02	82.34	74.74	78.36	1.95	1	82.17	71.66	76.56	3.41	1	82.12	71.77	76.60
	MaPLe	83.87	75.77	79.61	99.95	0	0.03	84.23	78.47	81.25	8.22	1	83.51	75.01	79.03	5.30	1	83.94	77.01	80.33
	PromptSRC	86.29	78.24	82.07	99.89	0	0.01	86.00	77.93	81.77	1.78	1	86.81	77.01	81.62	3.19	1	86.79	81.29	83.95

D.2 Experiments on More Datasets

We conducted extensive evaluations on 11 datasets, which covers a wide range of recognition tasks, including ImageNet [49] and Caltech101 [45] which consists of generic objects; OxfordPets [50], StanfordCars [61], Flowers102 [62], Food101 [63], and FGVC Aircraft [64] for fine-grained classification, SUN397 [65] for scene recognition, UCF101 [66] for action recognition, DTD [67] for texture classification, and EuroSAT [68] which consists of satellite images. All other settings remain consistent with our main experiments.

For evaluation, we use the harmonic mean (HM) between base and novel class accuracy, which represents generalization performance. In addition to SWAP, independent prompt, and independent verification

classes scenarios, we tested the accuracy of SWAP under normal usage conditions, *i.e.*, SWAP’s accuracy when verification classes are not included in the test classes, denoted as SWAP (no Veri).

As shown in Table D3, Experimental results demonstrate that our method maintains high accuracy on both base and novel classes across all datasets, while simultaneously achieving high WSR and small p-values. In the SWAP (no Veri) scenario, both base and novel class accuracies remain high, indicating that our method does not impair normal user experience. In independent prompt and independent verification classes scenarios, the WSRs are all below 10% and the p-values are relatively large across all datasets.

Appendix E Reproducibility Statement

The detailed configurations of datasets, models, hyperparameters, and computational resources are provided in Section 5 and Appendix C. The full implementation of our methods (including codes and model checkpoints) will be released upon the acceptance of this paper.